GEOLOGICA CARPATHICA, 2026, 77, 2, 115–136 https://doi.org/10.31577/GeolCarp.2026.06

Travertine bodies in the Dudince Spa: Indicators of multiple Quaternary reorientation of the paleostress field (Central Slovak Neogene Volcanic Field)

JÁN BÓNA[1,2,✉], JOZEF HÓK[3], KATARÍNA BÓNOVÁ[2], MICHAL GALLAY[2], JÁN DZÚRIK[4], JURAJ LITTVA[5], JURAJ TOMANA[4] and RASTISLAV VOJTKO[3]

[1]DPP Žilina Ltd.,Vysokoškolákov 1758/3, 010 01 Žilina, Slovakia
[2]Institute of Geography, Faculty of Science, Pavol Jozef Šafárik University in Košice, Jesenná 5, 040 01 Košice, Slovakia
[3]Department of Geology and Palaeontology, Faculty of Natural Sciences, Comenius University in Bratislava, Mlynská dolina, Ilkovičova 6, 842 15 Bratislava, Slovakia
[4]GEOSPEKTRUM Ltd., Mliekárenská 10, 821 09 Bratislava, Slovakia
[5]State Nature Conservancy of the Slovak Republic, Slovak Caves Administration, Hodžova 11, 031 01 Liptovský Mikuláš, Slovakia

(Manuscript received April 8, 2025; accepted in revised form February 24, 2026; Associate Editor: Igor Broska)

Abstract: The Dudince Spa, which is located on the southwestern fringe of the Central Slovak Neogene volcanic field, is renowned for its thermomineral waters, enriched in CO_2 and H_2S. Historically, mineral water springs had been located on several travertine mounds; however, these are now inactive due to the extraction of mineral water through wells. This research focuses on the travertine formations within the spa, and considers them essential for understanding the Quaternary tectono-hydrogeological evolution, notably through the analysis of reorientations in the paleostress field. Leveraging high-resolution LiDAR (Light Detection and Ranging)-derived digital terrain models (DTMs) and geomorphometric analyses, this study evaluates the potential to identify travertine deposits (geobodies) partially concealed by vegetation, while clarifying their spatial distribution and genesis. These travertine mounds are located along the northwestern and northeastern rims of the NW–SE-oriented Gestenec Elevation, which is directly linked to the horst found in the pre-Cenozoic basement. The structure forms a barrier to the inflow of mineral water from the northeast. The tectonic evolution of this elevated structure is connected to a shift in the orientation of the stress field from a NW–SE to NE–SW (ENE–WSW) direction up towards a ESE–WNW (SSE–NNW) direction, which had been generated by dextral movement along the Central Slovak Fault System during the period between the Middle Pleistocene and the Holocene. Faults oriented in the NW–SE to NE–SW directions facilitate the upward flow of both mineral water and the juvenile carbon dioxide that saturates it. The applied methodology (geospatial analysis and field geological research) illuminates the dynamics of stress field rotation, influencing the tectonic and hydrogeological properties of the study area. The results highlight the efficacy of LiDAR mapping and geomorphometry in geological exploration beneath a dense vegetation cover, thus providing a model for similar studies in geothermal fields and tectonically-active regions worldwide.

Keywords: Western Carpathians, travitonics, travertine mounds, airborne LiDAR mapping, mineral waters

Introduction

Travertines and/or calcareous tufa are terrestrial sedimentary deposits of calcium carbonate that are chemically precipitated around springs, lakes, and streams. They are known for their remarkable morphological structure, as well as having a very limited lateral extent (e.g., Ford & Pedley 1996; Pentecost 2005). The number of studies devoted to "young" continental carbonates constantly increases worldwide. The research goals often overlap in these studies; however, they are focused mainly on stratigraphy and radiometric dating (Brilli & Giustini 2023; Vieira et al. 2023), paleontology and archaeology (Schäfer et al. 2007; Dabkowski 2014), sedimentology and geochemistry (Özkul et al. 2014; Claes et al. 2015; Mohammadi et al. 2019), paleoclimatology (Dramis et al. 1999; Faccenna et al. 2008; Ricketts et al. 2019; Mancini et al. 2021), hydrothermal and geothermal systems (Capezzuoli et al. 2018; Brogi et al. 2020), and active tectonic or neotectonics (Altunel 2005; Capezzuoli & Sandrelli 2006; Brogi et al. 2007, 2010; Mesci 2012; Ekizoğlu & Mesci 2025). The impact of seismic shocks on the facies development of travertine, including the anatomy of a travertine mound, have also been studied (e.g., Gradziński et al. 2014).

Terrestrial carbonates are typically deposited in proximity to thermal and/or non-thermal springs, which are closely associated with faults and fracture networks in the bedrock that provide the necessary paths for groundwater (Hancock et al. 1999; Brogi & Capezzuoli 2009; Mesci et al. 2008; Brogi et al. 2007, 2012, 2021; Nishikawa et al. 2012; Török et al. 2017, 2019; Andrić-Tomašević et al. 2024; Bóna et al. 2024; Abou

✉ corresponding author: Ján Bóna
jan.bona@dppzilina.sk

Elmagd et al. 2024). This means that the travertine deposition and tectonic activity are inseparable processes; therefore, the terrestrial carbonate geobodies are critical for understanding the tectonic evolution of the area. In areas of ongoing tectonic activity, fissures and dislocations control the location, size, and geometry of travertine accumulations.

The term "travitonics" was introduced into the literature by Hancock et al. (1999) to highlight the relationship between travertine deposition and faulting. This concept indicates that a proper understanding of the history of travertine depositional systems can provide significant insights not only into the age of tectonic activity associated with fault structures, but also into the characteristics of the studied area (Hancock et al. 1999; Altunel 2005; Altunel & Karabacak 2005; Uysal et al. 2007). Such insights are essential for neotectonic research, particularly in identifying faults that have been active during the Quaternary or within the current tectonic regime.

Moreover, the geometry and distribution of travertine geobodies reveal the pattern and orientation of the systematic joints or fractures. These discontinuities can be used as a stress indicator of the ongoing tectonic activity and the reconstruction of past tectonic stresses (Altunel & Hancock 1993; Mesci et al. 2008; Brogi et al. 2010, 2017, 2020; Mesci 2012; Van Noten et al. 2013, 2019; Çolak Erol et al. 2015; Török et al. 2017; Şengül et al. 2019; Bóna et al. 2024), although the deformation of the governing stress and the developed fracture system can be complex (Ruszkiczay-Rüdiger et al. 2020).

In this context, the travertine occurrences at the Dudince Spa in south-central Slovakia offer an important, but underexplored case study (Fig. 1). While previous research in the area has primarily focused on the hydrogeological properties and therapeutic value of the local mineral waters (Hynie 1956a, b, 1963; Vandrová et al. 1988; Bačová et al. 2016; Dzúrik et al. 2021), less attention has been given to the geological and tectonic processes linked to its terrestrial carbonates, as well as to the role of individual geobodies and their brittle deformation. Studying these aspects is crucial for documenting the region's tectonic history and understanding their potential as indicators of paleostress field dynamics, particularly in relation to the neotectonic activity of the Central Slovak Fault System (CSFS – Fig. 1A, Kováč & Hók 1993; Bóna et al. 2024).

Recently, Németh et al. (2023) interpreted the brittle deformation present in the Plio–Quaternary sediments of the studied

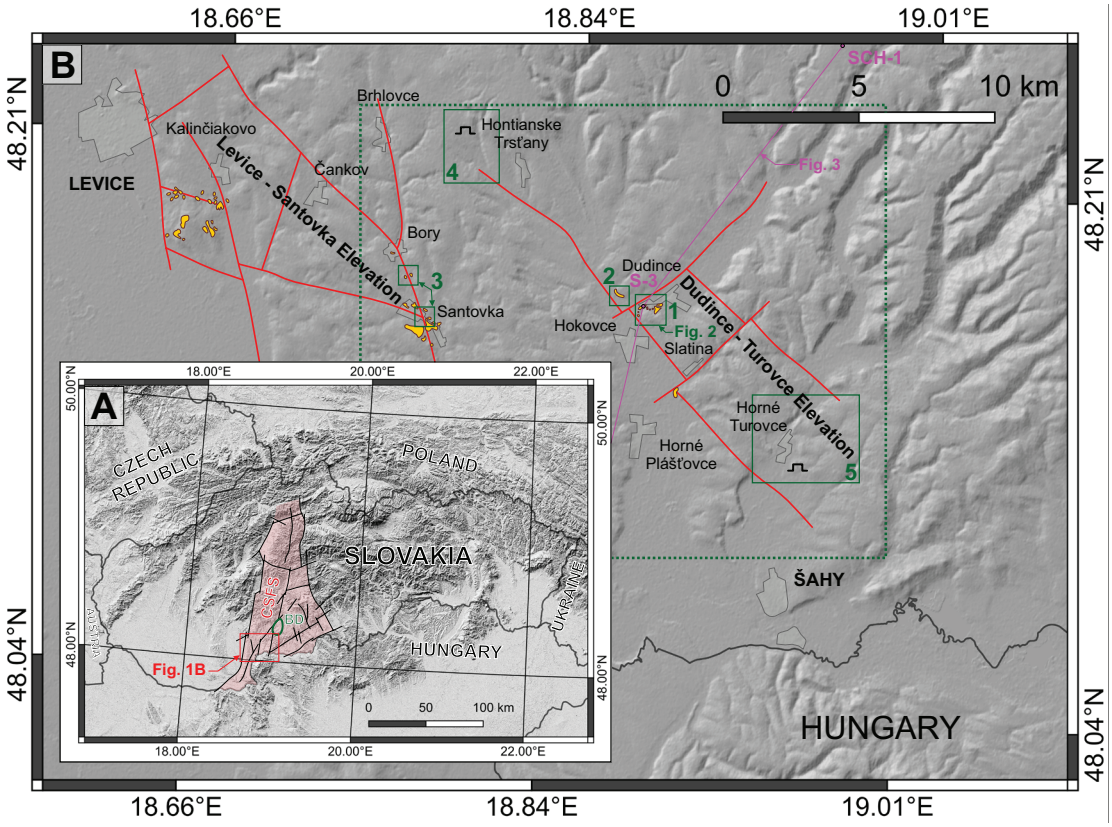

Fig. 1. (A) The position of the Central Slovak Fault System – CSFS (according to Hók et al. 2000, modified), green ellipse shows Bzovík Depression (BD). **(B)** Simplified structural scheme with the major faults (red lines) and the occurrence of travertines (yellow areas). Explanations: green dotted rectangle – morpholineament extraction area – linear valleys and scarps, green rectangles – studied areas: 1 – Dudince Spa and Gestenec area, 2 – Dudince village – Under the vineyards (Porošín – abandoned quarry), 3 – Búr river valley (north) and Santovka Spa (south), 4 – Hontianske Trsťany village – quarry (morpholineament extraction area – gully network), and 5 – Horné Turovce village – quarry (morpholineament extraction area – gully network).

area as a manifestation of the kinematic activity of regionally-significant shear zones during the final orogenic phase, which is referred to as AnD4. This interpretation raises important questions regarding the type of brittle deformation that occurred in the area during the Quaternary. In particular, uncertainties remain about the age, kinematics, and sequence of brittle deformation structures. Our study addresses this gap by integrating published and unpublished geophysical data, as well as new structural, geological, hydrogeological, and remote sensing data to develop a comprehensive model of the tectonic and hydrogeological evolution of the study area.

Additionally, it presents a novel, alternative perspective on the links between tectonic activity, travertine deposition, and subsequent brittle deformation.

This research aims to clarify the complex interaction between tectonic activity and travertine deposition, especially in the Dudince Spa area (Figs. 1 and 2), with an emphasis on understanding the various changes in the paleostress field during the Quaternary. By analysing the morphological and compositional characteristics of the travertine formations, we seek to refine the geological timeline of tectonic events and evaluate their impact on the hydrogeological systems of the Central Slovak Neogene volcanic field.

To achieve these objectives, we employ a comprehensive suite of methodologies, including field geological and structural mapping, paleostress analysis, high-resolution digital terrain modelling and geomorphometric analysis based on airborne LiDAR data, complemented by recently published radiometric ages of the travertine deposits by Vieira et al. (2023). These advanced techniques enable precise mapping of the travertine bodies concealed beneath dense vegetation, as well as a detailed analysis of their structural features, thereby providing new insights into their formation processes and development.

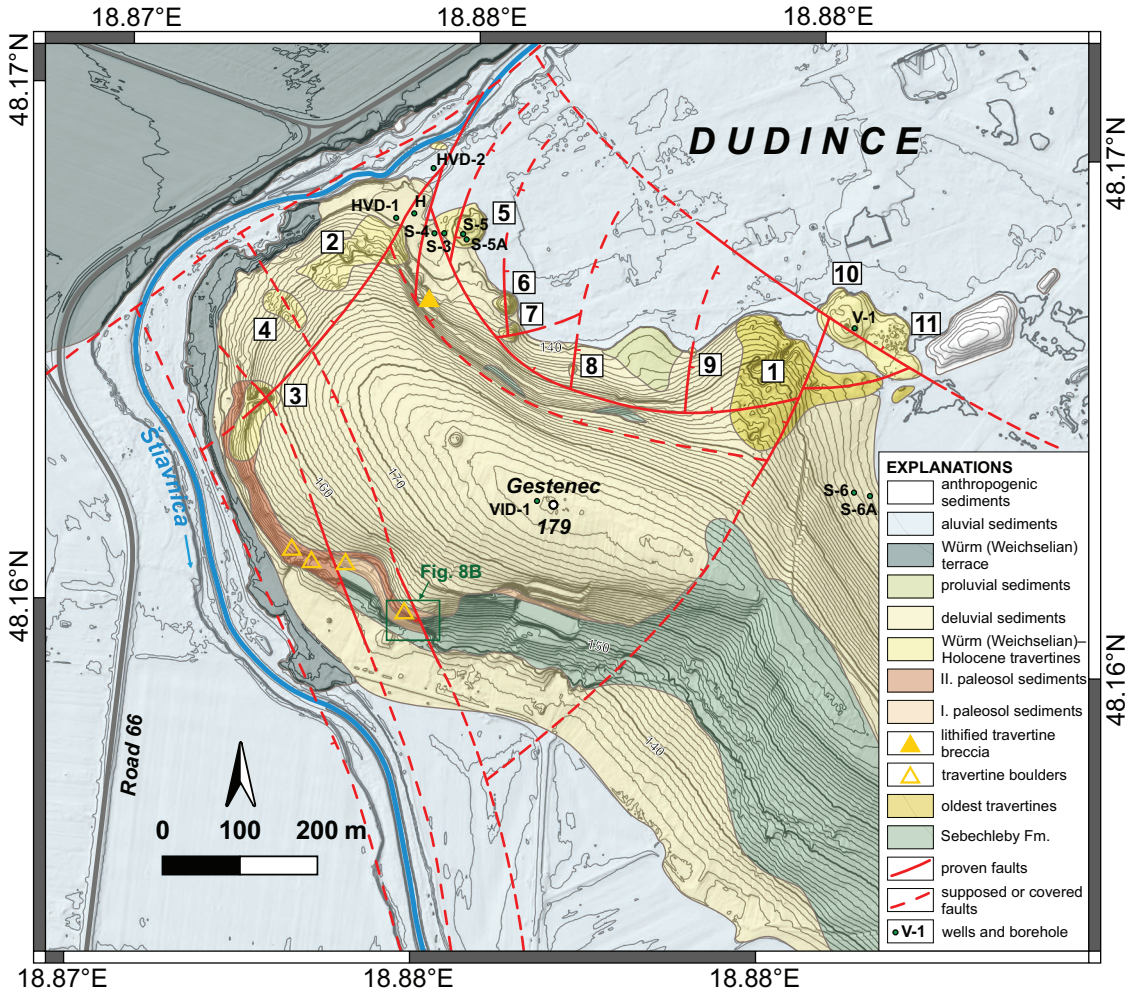

Fig. 2. Geological map (semi-transparent layer) of the Dudince Spa and Gestenec Elevation area with high-resolution topography visualization (hillshade with contoures – backing layer). The geological map is created according to own field observations and based on the interpretation of digital terrain analysis on LiDAR DTM (ZBGIS Map Client 2017). Numbers indicate individual occurrences of travertine geobodies (mounds): 1 – travertine at the amphitheatre, 2 – travertine at the swimming pool and surroundings, 3 – travertine at the abandoned quarry, 4 – tufa mound, 5 – Kúpeľný prameň Spring, 6 – Hostečný prameň Spring, 7 – Tatársky prameň Spring, 8 – Šípková Ruženka Spring, 9 – Očný prameň Spring, 10 – Grófsky kúpeľ Spring, and 11 – Rímsky kúpeľ Spring.

Geological and hydrogeological settings

The Dudince Spa area is located near the NE border of the Danube Basin and Štiavnica stratovolcano (Vass et al. 1988a). Although it is renowned for its exceptional healing water (Hynie 1963), it is also known for the occurrence of unusually well-preserved travertine mounds.

The geological structure of the Dudince Spa area is depicted on geological maps at a scale of 1:50,000 (Konečný et al. 1998; Nagy et al. 1998). The names of the Quaternary periods are indicated on these maps in accordance with the stratigraphic subdivision of the Quaternary in the Alps. However, the following text also contains the equivalents/periods used in Northern Europe.

Travertines are located on the northeastern and northwestern slopes of the NW–SE oriented morphological Gestenec Elevation (179 m a.s.l.), directly linked to the pre-Cenozoic basement horst structure (Fig. 2). The horst structure was referred to as the Levice spring line (Melioris & Vass 1982; Hyánková & Melioris 1993), also as the Turovce–Levice Horst (Vass et al. 1988b) or the Turovce Horst (Konečný et al. 2003). Recently, it was split into two separate elevations (Fig. 1B) – the Levice–Santovka Elevation and the Dudince–Turovce Elevation (Hók et al. 2020, 2021) – based on differences in their lithostratigraphic and tectonic composition. The pre-Cenozoic basement of the Dudince–Turovce Elevation is overlain by the lower Badenian Turovce Formation, which consists of terrigenous conglomerates representing the Neogene basal sediments (Vass in Melioris & Vass 1982). The middle Badenian Sebechleby Formation, which is composed of volcanic siltstones with intercalations of sandstones and conglomerates, marks the terminal sequence of the Neogene sedimentation (Fig. 2).

Quaternary deposits covering the Miocene sediments are represented by sediments of river terraces and floodplain of the Štiavnica River, colluvial (slope debris) sediments, and travertine (Fig. 2). Travertine bodies are defined as spring mounds and coalesced mounds (Pivko & Vojtko 2021). The macrophyte and microphyte facies of selected geobodies of calcareous tufas and travertines were studied by Pivko (2021).

The age of travertine ranges from the Lower Pleistocene to Holocene (Ivan 1943; Kovanda 1971; Halouzka 1977; Schmidt 1977; Franko 2001; Vieira et al. 2023).

The NE–SW directed extensional axis of the stress field played a significant role in the formation of the Levice–Santovka and Dudince–Turovce elevations during the Lower Badenian (Nemcok et al. 1998). The elevations acted as a barrier to gravity currents of volcanoclastic material descending from the Štiavnica stratovolcano, which is located approximately 30 km to the NNE, and prevented them from developing into turbidity currents. During the periods of the Pliocene and Lower Pleistocene, the paleostress field extension was oriented in the NE–SW direction. This extension conditioned the reactivation of faults in the NW–SE direction, as indicated by the pre-basaltic relief in the Cerová vrchovina upland, together with the NW–SE oriented palaeo-river valleys and the configuration of the river terraces (cf. Vass 1971; Vass et al. 1993).

Wachtel (1859) described two springs on the right bank of the Štiavnica River, likely referring to Pliocene travertine mounds in the Porošín area, which is approximately 1.5 km northwest of the study area. In addition, he noted seven springs on the left bank and several other springs in the meadow, although the number and specific locations were not provided. From 1917 to 1918, the ŠH-1 well (later referred to as "H") was drilled to a depth of 60 m, yielding 6 l/s. At that time, the majority of natural springs had already disappeared. The complete cessation of all natural springs occurred following the drilling of the S-3 well in 1954, which provided 70–80 l/s (Hynie 1963). The geological structure of the Dudince Spa area was intensively studied due to its hydrogeological conditions and the chemical composition of its mineral water (Hynie 1956a, b; Melioris et al. 1986; Vandrová et al. 1988; Bačová et al. 2015, 2016; Dzúrik et al. 2021). In general, the thermal water at the Dudince Spa is highly mineralised, containing carbon dioxide and sulfane while a wide range of main anions and cations contribute to the mineral composition. According to Palmer–Gazda's classification (Gazda 1971), the water is of a mixed type, with the predominant presence of calcium–hydrogen carbonate components. In abbreviated notation, the waters are classified as a mixed chemical type Na–Ca–(Mg)–HCO_3–Cl–(SO_4), with average mineralisation of approximately 5700 mg/l, a temperature range of 27–28 °C, and concentrations of free carbon dioxide between 1400–1800 mg/l and sulfane between 6–10 mg/l. Historically, there have been different opinions on the origin and circulation of the mineral waters (Maheľ 1952; Hynie 1956b; Melioris & Vass 1982; Hyánková & Melioris 1993). The specific mineral water at the Dudince Spa was considered to be a part of the Levice spring line, although this proposed line encompasses a variety of tectonic units, rock complexes, even different types of mineral waters (Hók et al. 2020, 2021; Dzúrik et al. 2021). The spring area is bound to the northeastern side of the Gestenec Elevation, representing a barrier (part of the Dudince–Turovce Elevation) to the inflow of mineral waters from the northeast (Fig. 3). In order to fully understand the origin and circulation of these mineral waters, it is necessary to consider the geology and tectonics of the broader surroun dings of the Dudice Spa. One key factor in this context is the Bzovík Depression (Konečný et al. 2003), whose centre lies approximately 20 km northeast of the Gestenec Elevation. The borehole GK-4 (Bzovík), which was drilled in the depression, penetrated (in addition to the Upper Cretaceous sediments and Middle Triassic limestones) the Oligocene evaporite strata with a total thickness of 124 m at a depth of 988 m (Marková et al. 1972; Biela 1978). These sediments are the source of the sulfane found in the mineral water, while the Middle Triassic limestones contribute significantly to the formation and transport of mineral water in the Dudince area. The epiclastic sediments of the Turovce Formation are the second key collector for the generation and circulation of the water, where the mineral water finishing processes occur

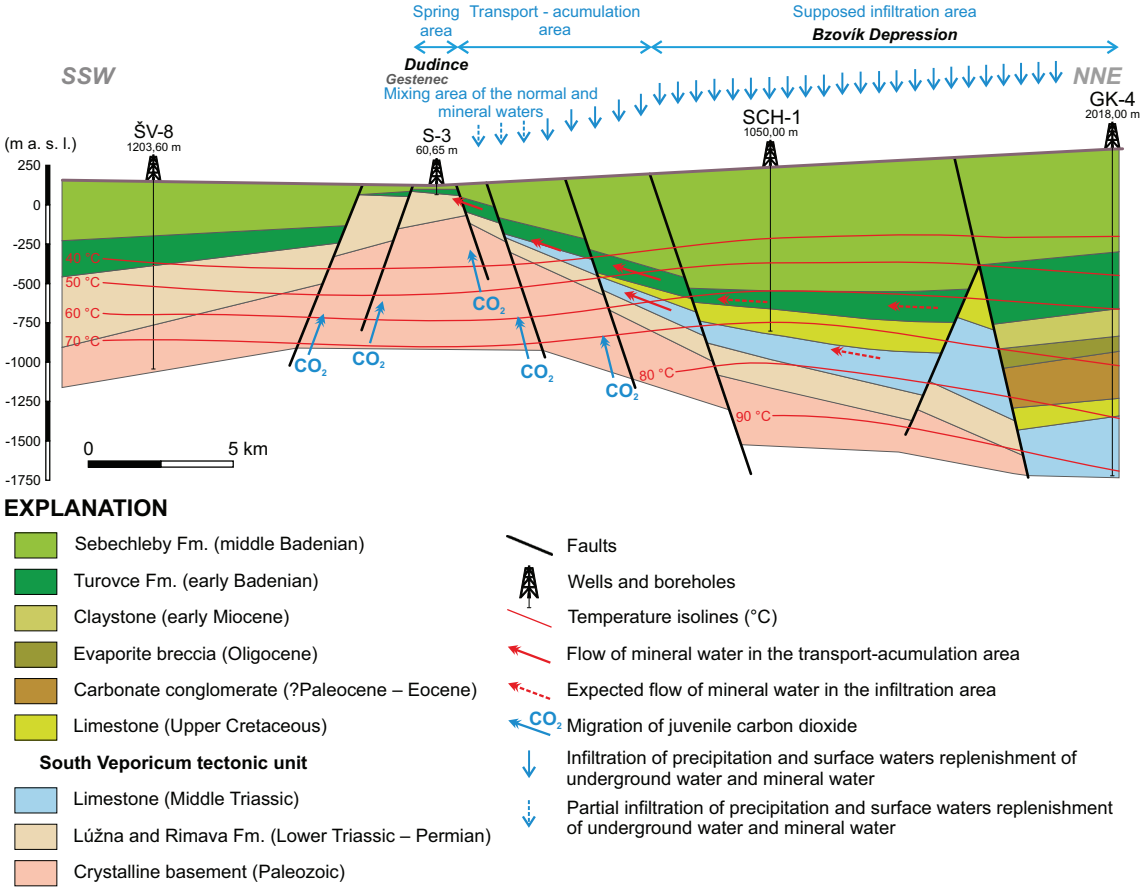

Fig. 3. Conceptual hydrogeological cross-section of mineral-waters structure in the Dudince Spa (Dzúrik et al. 2021, modified).

under a significant influence of CO_2. Juvenile carbon dioxide ascends along faults into the water-bearing Middle Triassic layers and the Turovce Formation (Dzúrik et al. 2021). Their influence is most intense in the northeastern marginal part of the Gestenec Elevation (Fig. 3).

Methods and data

The initial step in the research involved the systematic extraction of archival data, especially the results of drilling and geophysical studies. In essence, the structural configuration of the study area was derived from these extracted geodata, as well as from the results of geospatial analysis of a high-resolution digital terrain model (DTM) and data collected during field geological research.

Geomorphometric analysis

The objective of the geomorphometric analyses was to identify and characterise morphotectonic features in the Dudince Spa area and its broader surroundings. We focused on (i) mapping linear tectonic elements (morpholineaments) and (ii) detecting and delineating travertine mounds relative to their immediate non-travertine geomorphic context. This framing allowed for direct comparison of spatial patterns with independent constraints on Quaternary stress-field changes.

Analyses were carried out in QGIS v3.18.2 and v3.34 (QGIS Development Team 2020) with GRASS GIS 7.8 integration (GRASS Development Team 2020). Using the *r.param.scale* (Wood 1996) and *r.slope.aspect* (Hofierka et al. 2009) modules, we derived hillshade, slope angle, and multiple curvature measures following established theory on land-surface curvature (Evans 1972; Krcho 1973, 1983, 1990; Mitášová & Hofierka 1993; Shary 1995; Evans & Minár 2011; Florinsky 2016, 2017; Minár et al. 2020, 2024; Minár & Feciskanin 2024). More specifically, we computed *normal contour curvature* – $(k_n)_c$ (Krcho 1983; Minár et al. 2020), which is also called *horizontal curvature* – k_h (Shary 1995; Florinsky 2016, 2017) or *tangential curvature* (Mitášová & Hofierka 1993); *normal slope line curvature* – $(k_n)_s$ (Krcho 1983; Minár et al. 2020) also named *vertical curvature* – k_v (Shary 1995; Florinsky 2016, 2017) or *profile curvature* (Mitášová & Hofierka 1993); *maximal curvature* – k_{max} and *minimal curvature* – k_{min} (Shary 1995; Florinsky 2016, 2017; Minár et al. 2020). To further characterise terrain form, we computed *terrain closeness* and *topographic openness* (Yokoyama et al. 2002) and produced *diffuse-illumination* visualizations using the Relief Visualization Toolbox plugin for QGIS (Zakšek et al. 2011). This workflow supported mapping of

morpholineaments and delineation of convex, dome-like travertine mounds relative to their geomorphic context.

Geospatial data for the geomorphometric analyses were obtained from the Slovak Geodesy and Cartography Office via the ZBGIS Map Client (2017). The primary dataset was a 1×1 m gridded digital terrain model (DTM) derived from airborne laser scanning (ALS, LiDAR) point clouds collected during the national campaign in the spring of 2018. LiDAR acquisition in the leaf-off season enhanced terrain analysis because LiDAR pulses more readily penetrated the vegetation cover to reach the ground surface. Orthorectified satellite imagery is frequently used to support morphotectonic research (Heddi et al. 1999; Ahmadi & Pekkan 2021; Shebl & Csámer 2021), while geomorphometric modelling commonly relies on extracted digital Elevation models (Florinsky 2023). However, high-resolution airborne LiDAR enables precise quantification of land-surface properties beneath vegetation and, when combined with geomorphometric techniques, is highly effective for identifying tectonic linear features (DeLong et al. 2010; Lin et al. 2013; Pánek et al. 2020; Kania & Szczęch 2023; Sun et al. 2022).

The resulting raster maps were used to (i) extract morpholineaments (sensu Minár & Sládek 2009), thus linear trends of elongated forms and sharp, linear breaks in average landform properties and (ii) detect and delineate travertine mounds as convex, dome-like features relative to the surrounding terrain, defined here as the adjacent non-travertine geomorphic units (valley floors, slopes, erosional benches/terraces, alluvial–colluvial surfaces, and bedrock ridges) against which the mounds are contrasted. Features with atypical morphology or metrics were flagged as anomalous morphological elements for targeted field verification.

To complement the 2D DTM-based analyses, we used CloudCompare v2.12.4 (EDF & Telecom ParisTech 2007) to measure the dimensions and volumes of travertine mounds from the 3D LiDAR point cloud. These 3D metrics refined our understanding of mound morphology and scale and informed the structural-tectonic interpretation incorporated into the updated geological map of the Dudince Spa and wider region (Fig. 2).

Field geological research

Standard methods and techniques of geological mapping were used on a scale of 1:10,000 (e.g., Marko et al. 2007; Coe et al. 2010). Structural mapping was primarily focused on data collection and analysis of brittle structures.

We focused on mesoscopic discontinuities – faults and, in particular, systematic joints identified in the Mesozoic and Cenozoic bedrock (in the active quarries), as well as in travertine deposits (in natural outcrops or abandoned quarries), where their neotectonic character is indisputable. We determined the successive relationships of the tension joints and/or faults (older system/younger system) and then deformational phases (D1, D2 and D3).

The orientation of the horizontal stress field (minimum principal stress axis – S_{hmin}) was inferred through structural and paleostress analysis based on fault geometry and kinematics (Petit 1987; Angelier 1994; Dunne & Hancock 1994), as well as the spatial characteristics of the joints and open fissures (Hancock & Engelder 1989; Hancock 1991; Dunne & Hancock 1994; Stewart & Hancock 1994) following Hancock's concept based on a simple principle, where extension joints form normal to the minimum principal stress direction.

According to the key principles of "travitonics" (Hancock et al. 1999; Brogi et al. 2021), we assumed that the isolated spring fluids or travertine bodies are preferentially located along fault traces. We also assumed that neotectonic movements at the normal faults which are generally parallel to the direction of the riverbed, would have an impact on the river valleys by asymmetric development of river terraces (e.g., Cox et al. 2001; Viveen et al. 2012).

In the text, the orientation of measured planar structures (bedding planes, faults and joints) is given in dip direction/dip format in degrees (e.g., 220/80°), with the strike (azimuth) of the planar structure perpendicular to the dip direction. Joint measurements were statistically evaluated in the bidirectional rose diagram using GeoRose 0.5.1 software (Yong Technology Inc. 2014) plotting diagrams used in structural geological research.

Analysis and interpretation of the obtained data

Mapping travertine formations based on remote sensing and geomorphometry

Guided by geomorphometric theory, we evaluated which DTM derivatives best capture the convex signatures of travertine mounds. High-resolution airborne LiDAR-derived DTMs enabled systematic analysis of otherwise inaccessible ground (steep slopes, restricted areas) and the detection of landforms beneath forest canopies (Figs. 4A, 5A). A multi-parameter geomorphometric workflow is advantageous because different derivatives capture complementary aspects of mound morphology: curvatures emphasize convexity and rim–floor transitions, local slope angle highlights and measures mound-flank steepness, openness/closeness highlight local relief relative to the background surface, and diffuse-illumination variants enhance subtle edges. The efficacy of these parameters for recognizing convex-up, dome-shaped features is consistent with prior applications to volcanic edifices (Fornaciai et al. 2012; Pedersen & Grosse 2014), earth-mound fields (Sales et al. 2021), and burial mounds (Guyot et al. 2018; Vinci & Vanzani 2025). Applying multiple derivatives increases sensitivity under partial vegetation canopy reduces false positives from non-travertine convexities, as well as standardizes boundary placement across sites. The resulting quantitative metrics-planform geometry, height, volume, and relief contrasts-enable reproducible comparisons among mounds as well as through time, and provide a robust framework for

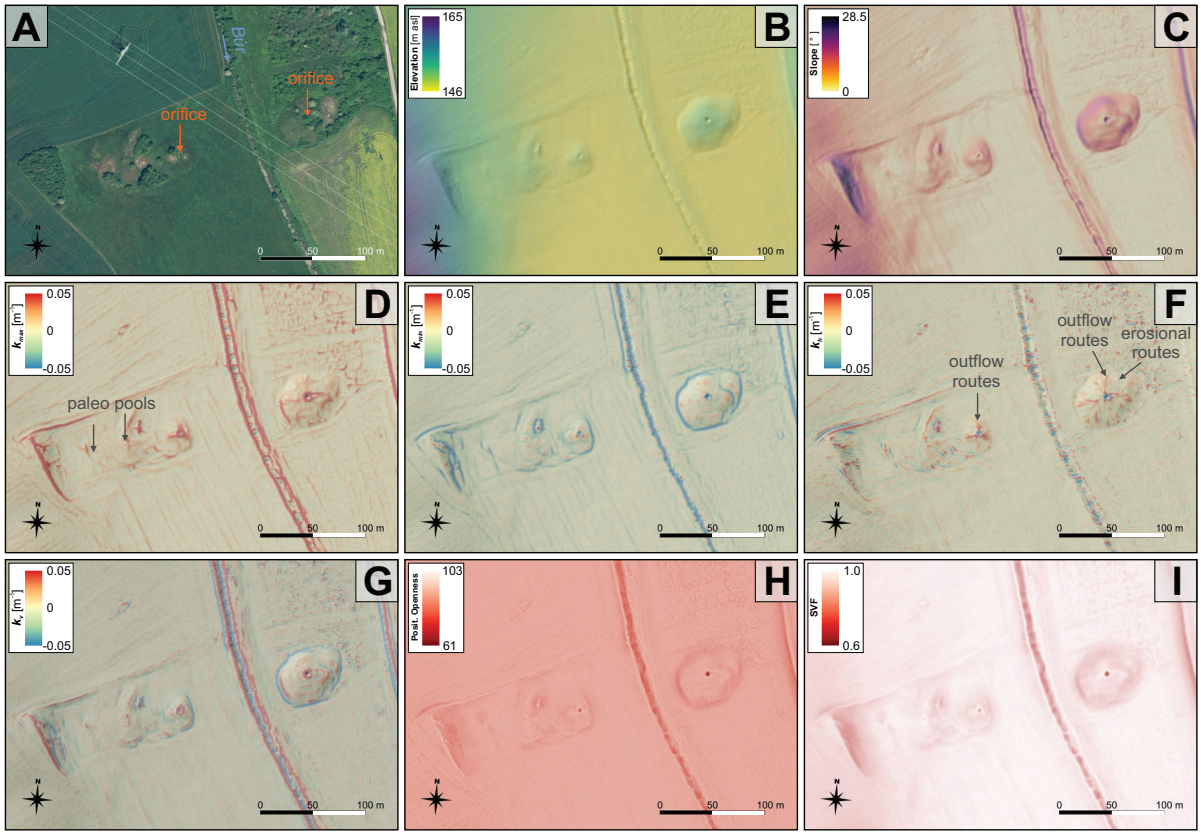

Fig. 4. Mapping of the travertine mounds (geobodies) of the Búr River valley (Budzgov meadows): **(A)** ortophotomosaic; **(B)** colour-shaded relief visualization; **(C)** slope angle (*S*); **(D)** maximal curvature (k_{max}); **(E)** minimal curvature (k_{min}); **(F)** tangential (horizontal) curvature (k_h) ; **(G)** profile (vertical) curvature (k_v); **(H)** positive opennes; **(I)** sky view factor (*SVF*).

testing spatial associations with morpholineaments and, in turn, evaluating Quaternary paleostress reorientations. The results indicate that for identifying various convex forms of travertine mounds in DTM, the application of second-order derivatives (curvatures – Fig. 4D–G; Fig. 5G–J) is more effective than mapping first-order derivatives (slope angle – Fig. 4C) or visualization using shaded relief (Figs. 4B, 5B).

The positive values of k_{max} and k_v accentuate the convex–concave curvature of the orifice, which represents the original vent of the travertine mound (Fig. 4D, G). Conversely, negative values of all four types of curvatures k_{max}, k_{min}, k_h and k_v (Fig. 4D–G) assist in identifying the concave-concave floor of the orifice (currently inactive). Negative k_{max} values indicate the remains of travertine pools, which appear as subtle, yet still concave-concave forms, as described by Ivan (1952) on the western mound (Fig. 4D). The curvature of a normal section, tangential to the contour line (horizontal curvature, k_h), identifies the divergence and convergence of gravity-drive surface flow (Krcho 1973). More specifically, $k_h>0$ indicates the outflow routes from the originally active central mouth of the travertine mound because mineral-rich waters, mainly dissolved calcium carbonate, built convex surfaces. $k_h<0$ indicates the routes created by rain that eroded the mound (Figs. 4F and 5I).

In principle, the application of the profile (vertical) curvature – k_v (Evans 1972; Krcho 1973; Shary 1995; Minár et al. 2020) is well-suited for identifying mound-shaped travertine deposits, which consist of numerous local convex and concave forms. This morphometric variable more sensitively and comprehensively characterises the specific geometry of the travertine geobodies (Figs. 4G and 5J). Within the dome-like morphology of travertine mounds, concave ($k_v<0$) and convex ($k_v>0$) landforms alternate, which may indicate the stacking of one travertine lobe on top of the other.

Positive openness (Yokoyama et al. 2002) and Sky View Factor (SVF; Zakšek et al. 2011) emphasize extremely occluded or exposed locations in the DTM (Figs. 4H and 5C, E; 4I and 5D, F). As implied by the definition, the "positive" convention follows that of terrain-slope curvature (sensu Pike 1988), whereby positive curvature denotes a convex-upward surface. Compared to openness, SVF provides a higher-contrast representation of terrain features. While openness is effective for detecting abrupt changes in topography (Figs. 4H; 5C, E), SVF better identifies the overall shape and extent of travertine mounds visually (Figs. 4I; 5D, F). Interestingly enough, both visualisation techniques proved to be sensitive to negative anthropogenic forms (Fig. 5C, D) in the landscape, such as abandoned open-pit travertine quarries, excavation pits, or terrain modifications made during the construction of

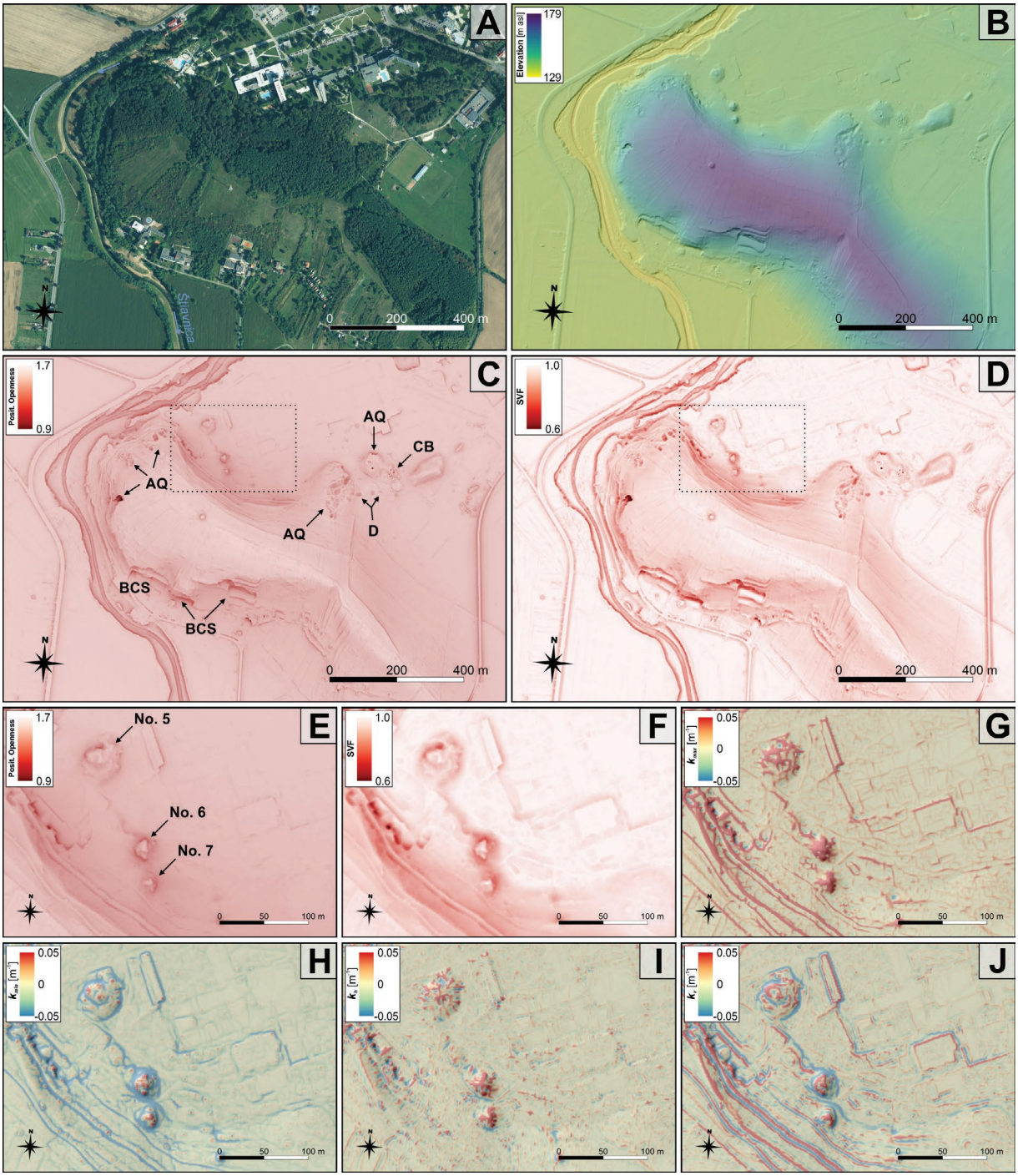

Fig. 5. Mapping of the travertine mounds (geobodies) of the Dudince Spa: **(A)** ortophotomosaic; **(B)** colour-shaded relief visualization; **(C)** positive opennes (Explanations: AQ – abandoned quarries, BCS – building cut slope, D – dolines, CB – carved bathtubs); **(D)** sky view factor (*SVF*); **(E)** black dotted rectangle C in detail (Explanations: travertine mounds: No. 5 – Kúpeľný prameň Spring, No. 6 – Hostečný prameň Spring and No. 7 – Tatársky prameň Spring); **(F)** black dotted rectangle D in detail; **(G)** maximal curvature (k_{max}); **(H)** minimal curvature (k_{min}); **(I)** tangential (horizontal) curvature (k_h); **(J)** profile (vertical) curvature (k_v).

hotels and sports infrastructure (e.g., on the southern slopes of Gestenec hill). These features represent potential sites for the collection of geological and structural data, especially in areas where natural travertine formations have been partially removed or exposed.

LiDAR data provided an accurate and detailed 3D representation of the travertine mounds, enabling the calculation of their volume and surface area. However, this process becomes more challenging with other methods (e.g., photogrammetry, ground surveying) when the features are obscured by

vegetation, such as trees or shrubs. Figure 6 illustrates a vertical cross-section through mounds no. 6 and no. 7 (see Fig. 2), highlighting the occlusion caused by vegetation while still preserving the underlying topography captured by airborne LiDAR. The volume of a travertine mound derived from LiDAR data serves as a proxy for estimating the duration and intensity of past spring activity. This can be used to determine carbonate deposition rates, contributing to reconstructions of paleoenvironmental and hydrogeological conditions. Furthermore, volumetric comparisons between sites assist in geomorphological classification and can serve as valuable analogues for subsurface carbonate reservoirs in applied geology.

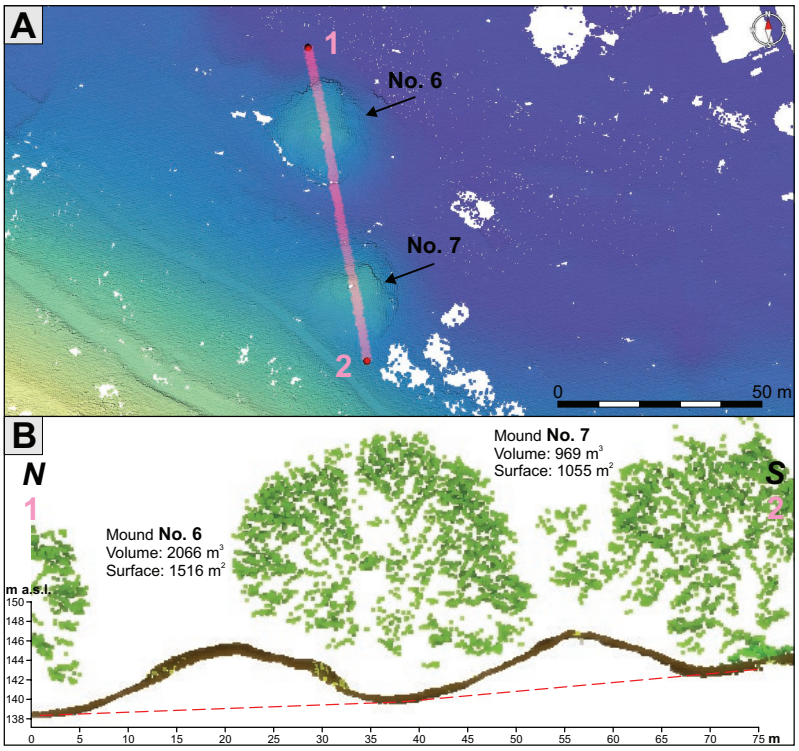

Fig. 6. Volumetric properties of travertine mounds (No. 6 – Hostečný prameň Spring and No. 7 – Tatársky prameň Spring, see Fig. 2) derived from a 3D LiDAR point cloud. **(A)** Planar view showing the location of the vertical cross-section, terrain elevation increases from blue to yellow; **(B)** vertical cross-section of the mounds with ground points is shown in brown and vegetation points in green. The volume was calculated for the 3D space between the ground points and the red dashed line representing the base plane for volume and surface area calculations.

Morpholineaments mapping

One of the objectives of morpholineament analysis was to identify structural trends in the broader area. In addition, we examined the relationship between linear geomorphological features, such as linear valleys, dells, low-relief scarps, and gullies, as well as brittle deformation structures, and used the results to supplement the structural dataset. Linear elements in the landscape, potentially of tectonic origin – morpholineaments – were interpreted from the raster layers of individual geomorphometric variables, including slope angle – S, tangential (horizontal) curvature – k_h and profile (vertical) curvature – k_v (e.g., Florinsky 1996, 2016; Jordan 2007). Important morpholineament trends, evaluated through bidirectional rose diagrams, were then compared with structural measurements and fault trends derived from geological methods.

The dominant trend of morpholineaments, obtained by delineation of the linear features, such as linear dells and scarps, shows an orientation ranging from NNW–SSE to NW–SE.

Gully networks have been mapped in the surrounding area of quarries, where pre-Plio–Quaternary bedrock sequences are exposed. The morpholineament rose diagram derived from the raster layer of the Hontianske Trsťany area (Fig. 7A) indicates that the predominant trends of lineaments are NE–SW (±45°) and WNW–ESE (±290°), with less significant trends oriented in the N–S (±360°) and ENE–WSW (±70°) directions. In the Horné Turovce area (Fig. 7B), morpholineaments in the NW–SE (±320°) direction with a wider dispersion are particularly prominent. The second transverse NE–SW (±40°) system is also clearly evident (Fig. 7B).

In general, Briestenský (2008), Burian et al. (2017), and Whitbread et al. (2024) do not report a direct, statistically-significant relation between fault strikes and spatial distribution of gully networks or erosion furrows. However, they do mention some local instances where a correlation between these features has been observed.

The dominant part of the analysed area is formed by various products of volcanic activity (lava flows, pyroclastics, epiclastics and volcanoclastics rocks), which are covered by eolian-colluvial and eluvial-colluvial sediments. Although lithology factors can determine the erodibility, permeability, and structural weaknesses of the terrain, which directly govern the initiation, orientation, and density of gully networks, we did not observe a causal relationship during the study of geological maps and field reconnaissance.

In this study, we tested the spatial relationship between neotectonic systematic joints and the orientation of the main trends of morpholineaments obtained by extraction from the system of gullies. Our results – a mutual comparison of geometry gully network and neotectonic joints trends – show that there is a strong spatial correlation between them.

The main trends of morpholineament concentrations (Fig. 7A, B) are parallel or sub-parallel to the measured systematic joints (Fig. 7G, H). This means that the relationship between the analysed datasets is not random; in other words, there is evidence that a real connection exists in the individual populations. In geomorphological terms, these structural

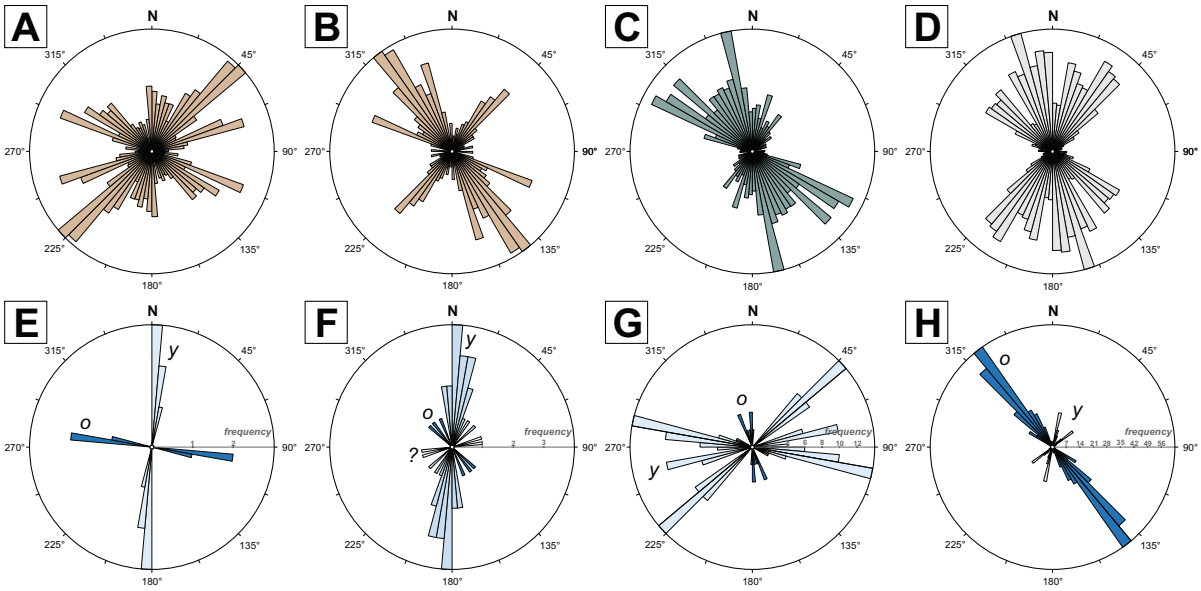

Fig. 7. Bidirectional rose diagrams of morpholineaments (A–D) and joints (E–H): **(A)** Hontianske Trsťany – quarry area; **(B)** Horné Turovce – quarry area; **(C)** linear valleys and scarps; **(D)** major regional faults extracted from the geological map; **(E)** Dudince village – Under the vineyards (Porošín – abandoned quarry); **(F)** Dudince Spa and Gestenec area; **(G)** Hontianske Trsťany village – quarry; **(H)** Horné Turovce village – quarry. Each interval in the rose diagram represents 5°, *y* – younger system of the tension joints, *o* – older system of the tension joints, *?* – without age determination. For locatisation of individual study areas (A to H) see Fig. 1B.

features (joint traces) act as erosional initiation zones or natural pathways that guide the surface flow and subsequently trigger gully formation and evolution.

In summary, we conclude that all statistically-systematic morphological features of the gullies (mainly orientation of the gully channel and spatial distribution of gully network pattern) indicate their tectonic origin because they are not random (cf. Scheidegger & Ai 1986). The orientation of drainage features or gullies often correlates with those of neotectonic joint sets.

Similarly, the major trends of identified morpholineaments (linear valleys and scarps; Fig. 7C**)** are parallel to several major regional faults (Konečný et al. 1998; Geological map 2008) that extend across the broader part of the studied area (Fig. 7D).

Geological mapping, structural data, and travitonics

Dudince village – Under the vineyards (Porošín)

An abandoned small quarry containing Pliocene-age travertine (Kovanda 1971) is located along the roadside, approximately 1.5 km WNW of the Dudince village centre. The bedding planes in the travertine display a shallow dip (10°) to the SE. The rock is disrupted by neotectonic systematic joints filled with calcite cementation (Fig. 8A), oriented in W–E (±280°, older system) and N–S (±5°, younger system) directions (Fig. 7E).

The axis of older S_{hmin} (deformational phase – D2) was oriented towards N–S, while the younger one was in the W–E (deformational phase – D3) direction.

Dudince Spa and Gestenec area

The findings from our new geological mapping indicate that the travertine geobodies are considerably less extensive (Fig. 2) than those depicted in the previously published geological maps (Konečný et al. 1998; Nagy et al. 1998; Geological map 2008). The travertine located on the northeastern and northwestern margins of the Gestenec Elevation (179 m a.s.l.) forms rather isolated mounds of various ages. Lithologically, two types of terrestrial carbonates were recognised: (i) compact grey-white to light-brown travertine (travertine at the amphitheatre, a part of travertine at the swimming pool, and travertine in the abandoned quarry – Nos. 1, 2, and 3 in Fig. 2, respectively); and (ii) porous, layered, often crumbly travertine, somewhere within the lithified flora residues.

Two fossil soil horizons have been identified on the southern and southwestern slopes of the Gestenec Elevation. The older horizon (I. paleosol sediments), which overlies the volcanic sediments of the Sebechleby Fm., consists of a rusty rubified soil layer (10–30 cm) overlain by brown soil containing pale volcanic clasts, with a maximum size of 3–5 cm. The second horizon (II. paleosol sediments), superimposed above the first horizon, consists of rubified soil at the base (10–30 cm) and brown to dark brown soil containing compact travertine clasts, which can reach sizes between 5 and 100 cm of the oldest travertine (No. 1 in Fig. 2; Fig. 8B). These paleosol horizons are likely to be genetically-associated with the river terraces, although their original position has been affected by younger normal faults (Figs. 2, 8B and 9). These observations indicate that a long-lasting hiatus occurred following

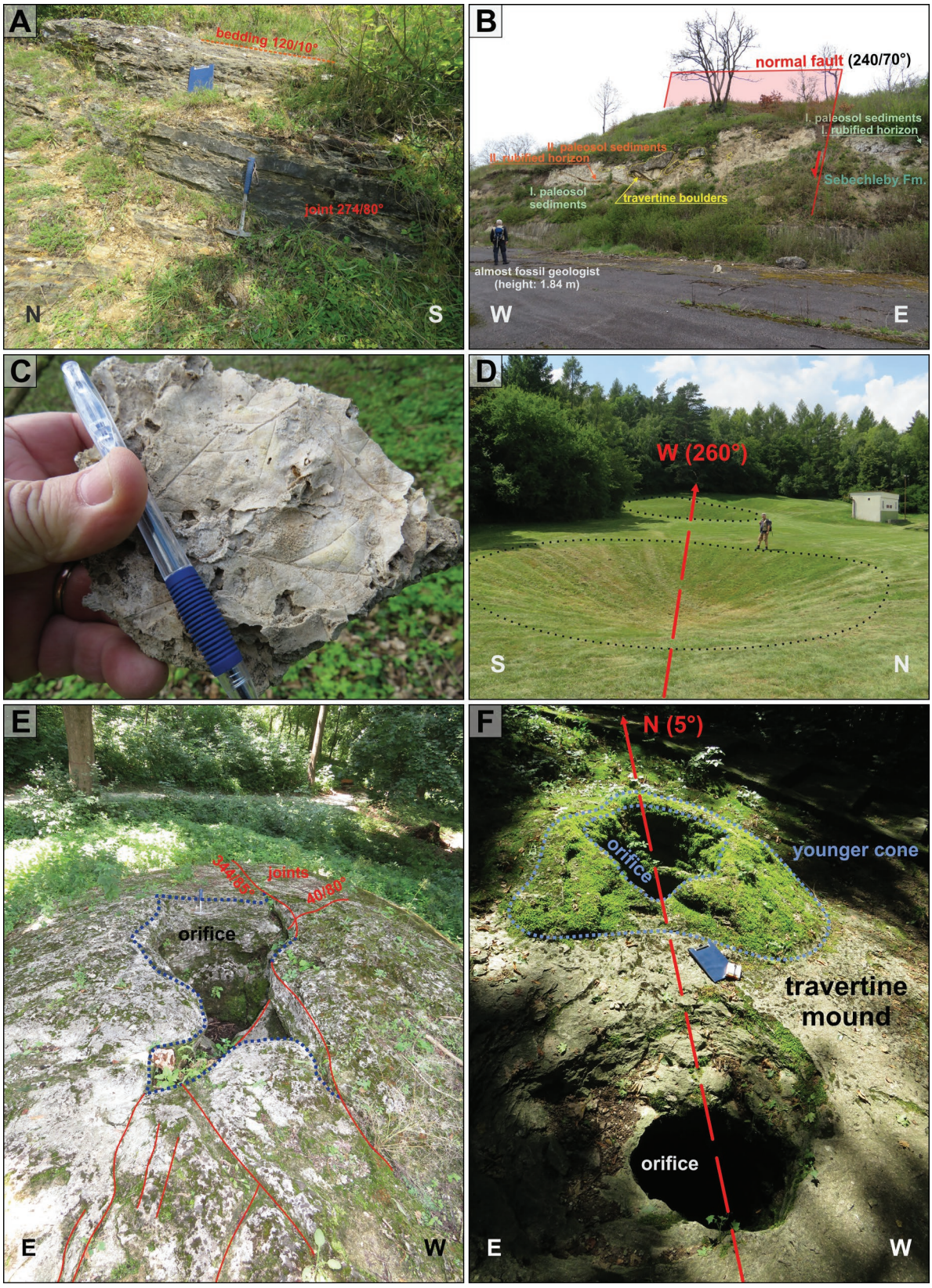

Fig. 8. (A) Joints in the travertine of the Pliocene age (Dudince village, Porošín – abandoned quarry); **(B)** fault segmenting two fossil soil horizons (S and SW slopes of the Gestenec Elevation) ; **(C)** fossil leaf impressions (*Quercus*), tufa mound No. 4; **(D)** the funnel-shaped dolines at the NE base of the Gestenec Elevation slope (red arrow shows azimuth); **(E)** Tatársky prameň Spring travertine mound (No. 7) disrupted by discontinuites; **(F)** Očný prameň Spring travertine mound (No. 9) consists of two orifices mound-type morphology (red arrow shows azimuth).

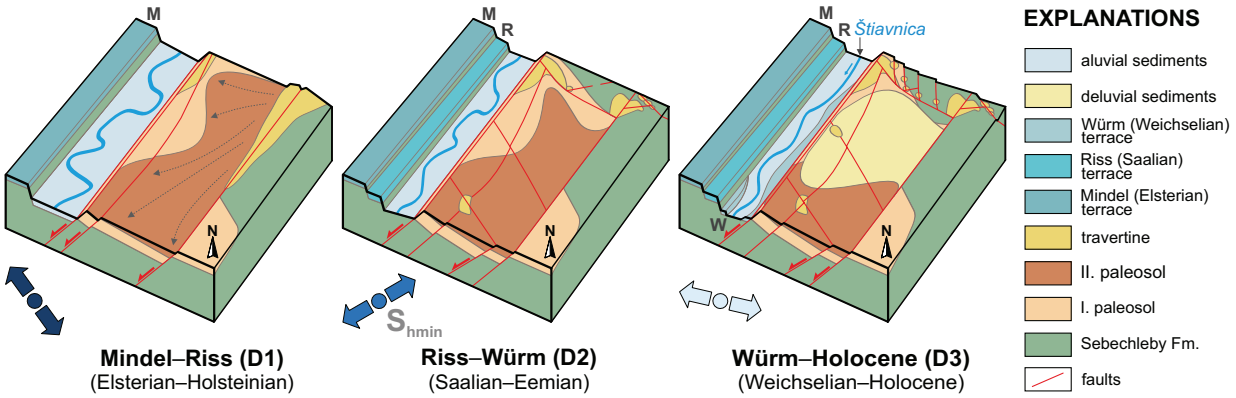

Fig. 9. Simplified tectonic evolution of the Dudince Spa and Gestenec area (geological structure according to Konečný et al. 1998; Nagy et al. 1998, simplified).

the deposition of the volcano-sedimentary complex of the middle Badenian Sebechleby Fm.

The oldest travertine mound (No. 1 in Fig. 2) was largely destroyed due to extensive exploitation in the past (Ivan 1943; Pilous 1973). However, remnants of the travertine are preserved in the local amphitheatre and its surrounding areas (Fig. 2). An incomplete molar of *Archidiskodon meridionalis* (Nesti) was described at this locality, dated to the end of the "Cromerian Interglacial" (Schmidt 1977). The travertines were later dated to the period 750–600 kyr (Franko 2001), which corresponds to the previous finding. The travertines overlie the Sebechleby Formation (Fig. 9).

Travertine at the swimming pool (and in its surroundings, No. 2 in Fig. 2) occupies a similar geological position, situated above the Sebechleby Fm. This mound was likely part of the travertine deposit and later covered by slope debris, as confirmed by the HVD-1, HVD-2, and S-4 boreholes (Vandrová et al. 1990a).

This occurrence consists of the remains of a travertine mound (Ivan 1943), which today exists only in the form of compact white travertine boulders dated to 450–350 kyr (Franko 2001), representing the Mindel–Riss or Holsteinian period.

Gravels and sandy gravels with well-rounded pebbles measuring 8–10 cm in diameter have been previously described below the crumbly travertine in the HVD-2 well (Vandrová et al. 1990b). The total thickness of the gravel layer is 7.0 m, and it most likely corresponds to the fluvial sediments of the Štiavnica River Würm–Holocene (Weichselian–Holocene). Given that the travertine in borehole HVD-1 directly overlies the volcanic sediments of the Sebechleby Fm., we interpret this travertine to be older than the crumbly travertine found above the Holocene fluvial gravels in borehole HVD-2.

We believe the formation of the oldest travertine mounds (travertine No.1 and No.2) to be associated with NE–SW oriented faults during the Mindel–Riss (Elsterian–Holsteinian) period, (NW–SE-directed S_{hmin}, deformational phase – D1), coeval with the formation of the Mindel (Elsterian) Terrace of the Štiavnica River (Fig. 9).

The travertine at the abandoned quarry (No.3 in Fig. 2) is compact and well-lithified. The Riss–Würm (Eemian) age was determined for this geobody (Franko 2001). Such information corresponds to the travertine presence (travertine boulders, Fig. 8B) above the higher, i.e., II. paleosol horizon most likely of Mindel–Riss (Holsteinian) age, which refers to the destruction of the first travertine mounds. The Riss (Saalian) terrace (Fig. 9) of the Štiavnica River likely formed concurrently with this travertine type. The tectonic activity occurred on the NW–SE faults during the Riss–Würm (Eemian) period, simultaneously with the faulting of paleosol horizons. The formation of travertine geobodies located northeast of the Gestenec Elevation at the Močidlá site (Grófsky kúpeľ Spring – No.10 and Rímsky kúpeľ Spring – No.11; Fig. 2) was also initiated during this period.

The tufa mound (No. 4 in Fig. 2), which is located between the No. 2 and 3 travertine occurrences, was most likely deposited on colluvial (debris slope) sediments. The tufa contains numerous fossil plant remnants, primarily leaf impressions, including those of *Quercus* (Fig. 8C). We propose that this tufa mound was formed during the early Holocene.

The Holocene travertine mounds, as well as those active throughout the Pleistocene to the Holocene, formed predominantly as spring mounds (*sensu* Pentecost 2005; Scheuer & Schweitzer 1985) with central orifices on the northeastern slope of the Gestenec Elevation (Kúpeľný prameň Spring – No. 5, Hostečný prameň Spring – No. 6, Tatársky prameň Spring – No. 7, Šípková Ruženka Spring – No. 8, Očný prameň Spring – No. 9, and travertine found in the HVD-2 well (see Vandrová et al. 1990b; Fig. 2). These travertine mounds represent individual depo-elements within the proximal zone of the travertine depo-system (*sensu* Mancini et al. 2019).

Although the Tatársky prameň Spring travertine (No. 7) has been dated to 301,072±18,317 yr BP and the travertines from the Močidlá site (Grófsky kúpeľ Spring No. 10) to the 25,853 ± 2124 yr BP (Vieira et al. 2023; Fig. 2), there are some historical records of their recent activity (Hynie 1956a); therefore, their formation was apparently a long-term process.

The NE–SW-striking faults can be considered the oldest faults in the studied area (Fig. 9). The fault along the course of the Štiavnica River valley exhibited activity as a normal fault dipping to the northwest. The ongoing activity of this fault is supported by the asymmetric development of the Mindel (Elster) and Riss (Saal) terraces (see Konečný et al. 1998; Nagy et al. 1998), which are located exclusively on the right bank of the river (Fig. 9). The Würm (Weichselian) terraces were formed along both banks of the Štiavnica River during the diminished tectonic activity of faults oriented in the NE–SW direction.

The paleosol horizons were probably formed during Mindel and Riss (Elsterian to Saalian) although it is possible that the lower horizon is older (possibly Lower Pleistocene). Both horizons are disrupted by normal faults generally oriented in the NW–SE (240/70°) direction and dipping to the southwest on the southwestern slope of the Gestenec Elevation (Figs. 2, 3 and 8B). The fault of similar orientation and kinematics was also detected geophysically by vertical electrical sounding (VES) on the southwest slope of the Gestenec Elevation (Tkáčová 1978).

The northeastern slope of the Gestenec Elevation is disrupted by normal faults oriented in the NW–SE direction and dipping to the northeast (Hynie 1956a). These faults are also clearly identified by VES (Tkáčová 1978). The fault oriented in the NW–SE to NNW–SSE direction can be inferred from the distinct geological conditions observed in the HVD-1, H, HVD-2, and S-4 wells (Hynie 1956a, b; Vandrová et al. 1990a, b). Neogene volcanic sediments drilled in S-5A and V-1 wells (Vandrová et al. 1988; Hynie 1956a) have been displaced downward along these faults by 27 m and 35 m, respectively, in comparison to surface exposures. In the V-1 well (see No. 10 in Fig. 2), a normal fault with an orientation ranging from WNW–ESE to NW–SE, dipping to the northeast, and exhibiting a total displacement of 10 m, was documented (Hynie 1956a, b).

The E–W (260°)-striking fault segmenting of the travertine mound (No. 1 in Fig. 2) is documented by the presence of several karst dolines at the NE base of the Gestenec Elevation slope. The funnel-shaped dolines were previously described by Pilous (1973), and their generally linear arrangement (Fig. 8D) indicates the presence of zones influenced by brittle tectonics (Veselský et al. 2014; Lačný et al. 2024).

The Riss–Würm (Eemian) travertine at the abandoned quarry (No. 3 in Fig. 2) is disrupted by older (NW–SE) and younger (NE–SW) systematic joints. The axis of older S_{hmin} (deformational phase – D2) was oriented in the NE–SW direction, and the younger deformational phase D3 was oriented in the NW–SE direction (Fig. 9).

Most of the Würm–Holocene (Eemian–Holocene) and recently active travertine is disrupted by N–S to NNE–SSW oriented systematic joints (Fig. 7F). One exception is the oldest Tatársky prameň Spring (No. 7) travertine mound, which is disrupted by a significant discontinuity in the ENE–WSW direction (Fig. 8E), as well as by joints oriented in the NW–SE and NNE–SW directions.

The Očný prameň Spring (No. 9 in Fig. 2) is composed of two orifices oriented in the N–S (5°) line. This observation suggests the mound-type morphology (Fig. 8F) of the travertine (Brogi 2004; Brogi et al. 2007, 2021), which develops along the fault trace. Thus, on the basis of the aforementioned information, the orientation of S_{hmin} (deformational phase – D3) can be reasonably inferred to be in the W–E to WNW–ESE direction.

Búr River valley and Santovka Spa

The Búr River valley (Fig. 1B) appears to follow the alignment of a fault oriented in the NNW–SSE direction. This dislocation was active as a normal fault, dipping to the east-northeast, and its activity can be indicated by the asymmetric development of the Riss (Saalian) terrace (Konečný et al. 1998; Geological map 2008), which is solely located on the left bank of the river (as well as by the distinct geological composition of the opposite slopes of the valley). The orientation of S_{hmin} is perpendicular, in the ENE–WSW direction (deformational phase – D2).

Two isolated travertine/tufa mounds are located between the villages of Santovka and Bory (Fig. 1B) in the area of the Budzgov meadows. These travertine geobodies are deposited directly on the original Holocene floodplain sediments, or on relatively younger travertine-enriched lake/swamp sediments (Šolcová et al. 2020).

Elongated (elliptical) central orifices (axis azimuth 60° to the ENE) of the individual mounds and an inactive parasite vent (Fig. 10A) on the eastern mound, as well as currently inactive isolated mineral springs (with pools, temperature up to 20 °C), which have been previously described by Ivan (1952), are oriented in a WSW–ENE direction, transversely to the valley. The orientation of the travertine mounds differs from the orientation shown on the geological map (Konečný et al. 1998; Geological map 2008).

Configuration of travertine geobodies and springs indicates the presence and course of younger, transversely-oriented tectonic dislocation of identical direction (Ivan 1952; Bondarenková 1983; Brogi et al. 2021). The aforementioned indicators, coupled with information from the reinterpreted profile No. 1 (Electrical Resistivity Tomography, Šolcová et al. 2020), suggest the presence of fault dipping toward the SSE direction.

A similar situation exists in the centre of the village of Santovka, where a travertine spring mound is a part of a complex of Cromer–Holocene travertine deposits (Halouzka 1977). The Holocene age of this travertine geobody has recently been confirmed by U–Th dating (7032±356, 6841±323, and 4808 ±1157 yr BP, respectively; Vieira et al. 2023). A dislocation of a similar orientation to the fault described in the previous paragraph beneath the travertine mound was proposed, based on the data from boreholes (Bondarenková 1983). Our observations indicate that the mound orifice has an elliptical shape, elongated in the direction of the fault, with an axis oriented at 60° to the ENE direction (Fig. 10B).

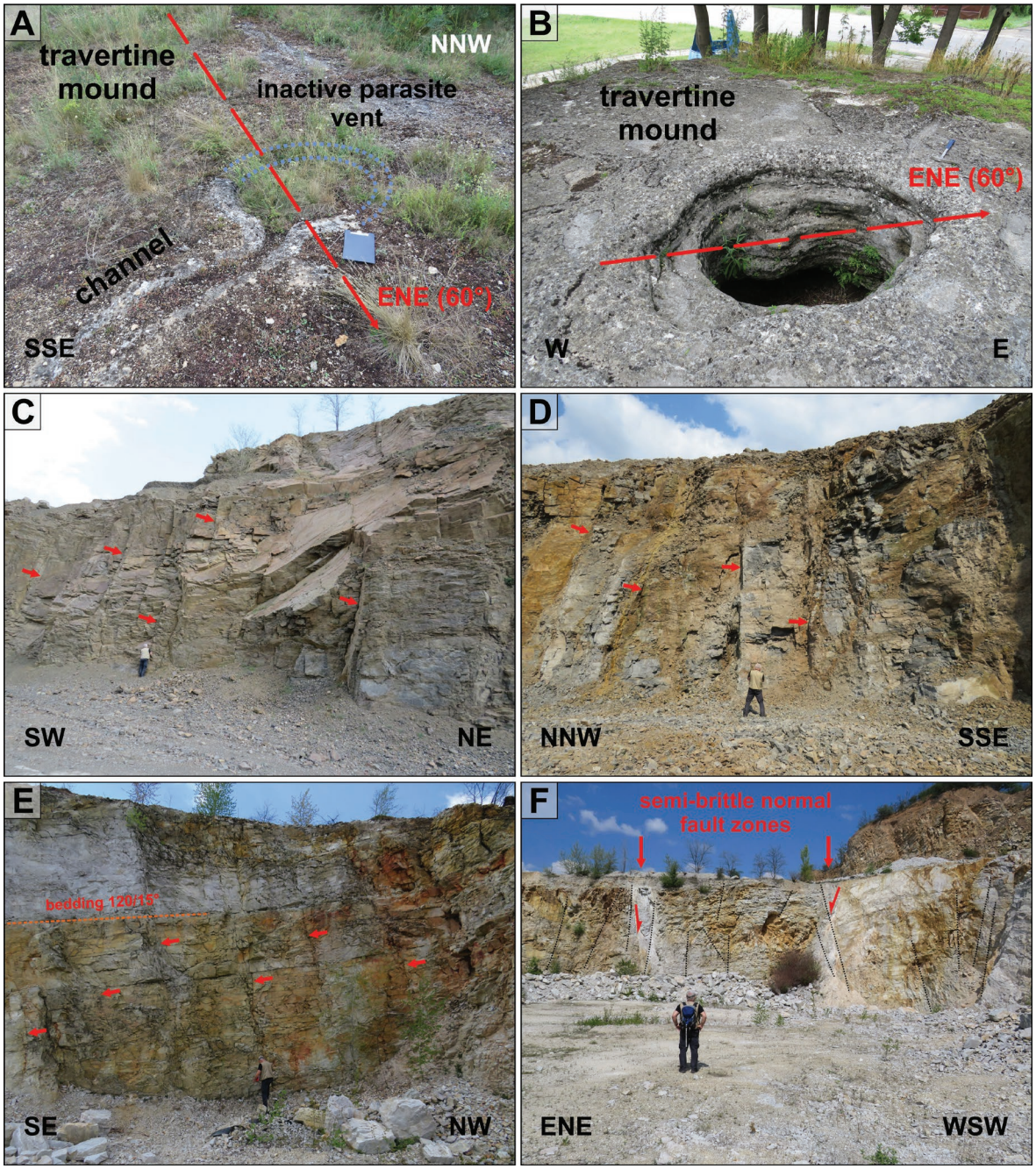

Fig. 10. (A) Inactive parasite vent on the eastern travertine mound (Búr River valley, red arrow shows azimuth from the mound orifice); **(B)** elliptical shape of the travertine mound orifice of the Holocene age (Santovka Spa, red arrow shows azimuth); Hontianske Trsťany village – quarry: **(C, D)** neotectonic joints (red arrow) cutting through the internal structure of the andesite lava flow body; village of Horné Turovce – quarry: **(E)** neotectonic joints (red arrow) cutting through the quartzites; **(F)** semi-brittle normal fault zones in the quartzites interrupted by younger systematic joints (black dotted line).

According to the normal faulting regime, S_{hmin} is oriented transversely in the NNW–SSE direction (deformational phase – D3).

Hontianske Trsťany village – quarry

Andesites of the Sarmatian age (Baďany Fm., Štiavnica stratovolcano, Konečný et al. 1998; Geological map 2008) are currently being extracted in the active quarry located approximately 2.5 km NW of the village of Hontianske Trsťany (Fig. 1B). Neotectonic joints intersect the horizontal, occasionally gently-inclined, platy jointing developed within the lava flow body, which is clearly visible in the quarry (Fig. 10C). Joints are mostly steep (80–90°) and show two separate trends. The first system can be interpreted as a spectrum of systematic vertical joints (Hancock 1968, 1991;

Hancock & Engelder 1989) comprising extension joints of an ENE–WSW (70–80°) direction and conjugate (hybrid) joints enclosing a range of dihedral angles of approximately 50–60° with a concentration of NE–SW (±50°) and WNW–ESE (±100°) orientations (Figs. 7G and 10D). The second conjugate system is represented by the two vertical sets of the dihedral angle, namely NNW–SSE (340°) and N–S (360°) orientations (Fig. 7G).

The orientation of neotectonic vertical extension and conjugate hybrid joints, as well as the formation order of neighbouring discontinuities (Dunne & Hancock 1994; Stewart & Hancock 1994) indicate the following paleostress results: The direction of extension (S_{hmin}) during older joints was oriented in an ENE–WSW direction (deformational phase – D2). Minimum principal stress (S_{hmin}) during the younger deformational phase D3 was generally oriented in a NNW–SSE direction.

Horné Turovce village – quarry

The Lower Triassic quartzites (Lúžna Fm. – south Veporicum, Konečný et al. 1998; Geological map 2008) belonging to the Dudince–Turovce Elevation (Hók et al. 2021) are extracted in the active quarry located approximately 0.5 km SE from the village of Horné Turovce (Fig. 1B). The bedding planes dip gently (10–20°) to the SE (Fig. 10E). The rocks exposed in this quarry are intensely fractured by systematic/neotectonic joints. Neotectonic joints are predominantly steep (75–80°), to sub-vertical (80–90°), with some having a locally gentler dip, and exhibit two distinct trends. The first system of joints can be interpreted as conjugate steep structures, as well as extensional structures (*sensu* Hancock 1968, 1991; Hancock & Engelder 1989) of the NW–SE (±320°) direction, with dispersion in the interval of 300 to 340° (Fig. 7H). The second conjugate system (Figs. 10E and 7H) is represented by two vertical sets of N–S (10°) to NE–SW (50°) orientations (with a dihedral angle of 40–45°).

Based on the orientation of neotectonic joints and faults, as well as the relative chronology of adjacent discontinuities (after Dunne & Hancock 1994; Stewart & Hancock 1994), the paleostress interpretation indicates that older tectonic structures formed perpendicular to NE–SW-directed extension (deformational phase D2), whereas younger structures developed perpendicular to the NW–SE-directed extension (deformational phase D3). Additionally, NW–SE-striking faults have been documented, dipping steeply to the NE or SW. Kinematic data indicates normal movements along these faults. Some of the normal faults-oriented NW–SE exhibit signs of semi-brittle (or brittle-ductile) deformation (Fig. 10F). Based on the developed brittle-ductile deformation, the origin of which is related to a temperature of ~300 °C (Scholz 2002), it is assumed that these faults originated in the Lower Miocene when the Turovce Elevation formed a barrier to the spread of volcaniclastic material (Vass et al. 1993) and faults could have been reactivated later (Nemcok et al. 1998). The faults are interrupted by younger systematic joints (Fig. 10F) of the same orientation, or approximately the same as those in younger Miocene volcanic formations and Plio-Quaternary travertines.

Discussion

The results (Figs. 9, 11, and 12) confirmed a change in the orientation of the extensional component of stress during the Quaternary period in the Internal Western Carpathians (Littva & Hók 2014; Littva et al. 2015; Hók et al. 2016; Bóna et al. 2024). During the Pliocene–Lower Pleistocene, the extension in the Internal Western Carpathians (IWECA) was oriented in the NW–SE to N–S direction, generally perpendicular to the IWECA arc. This orientation of the extension

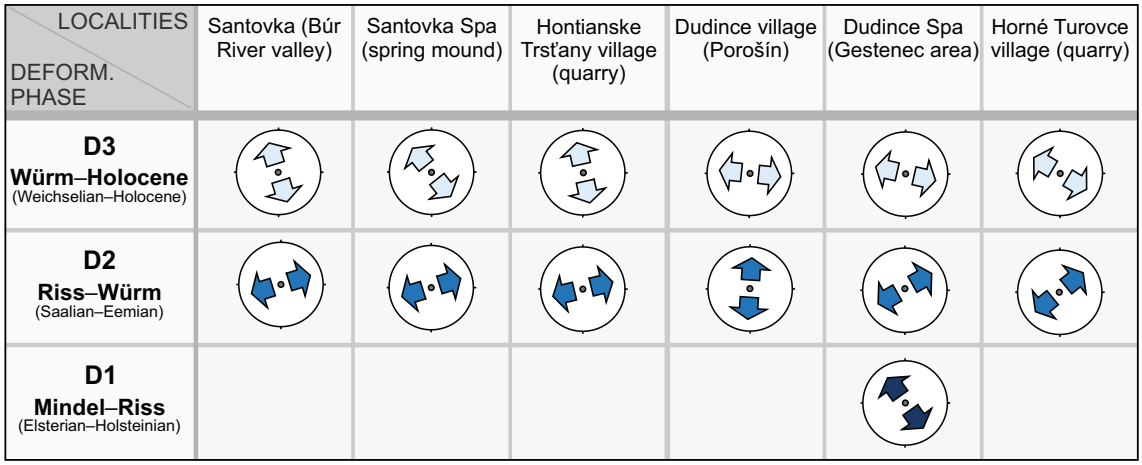

Fig. 11. Dudince region synthetic table of the Quaternary minimum regional horizontal stress (S_{hmin}). The orientation of S_{hmin} was derived mainly from the orientation of systematic subvertical parallel sets of joints, the formation of which requires effective tensile stress oriented perpendicular to the joint surface and low differential stress. Joints of proven origin due to gravitational breakdown of travertine mounds and cross joints (Hancock 1991) were recorded, but not included in determining the orientation of regional extension.

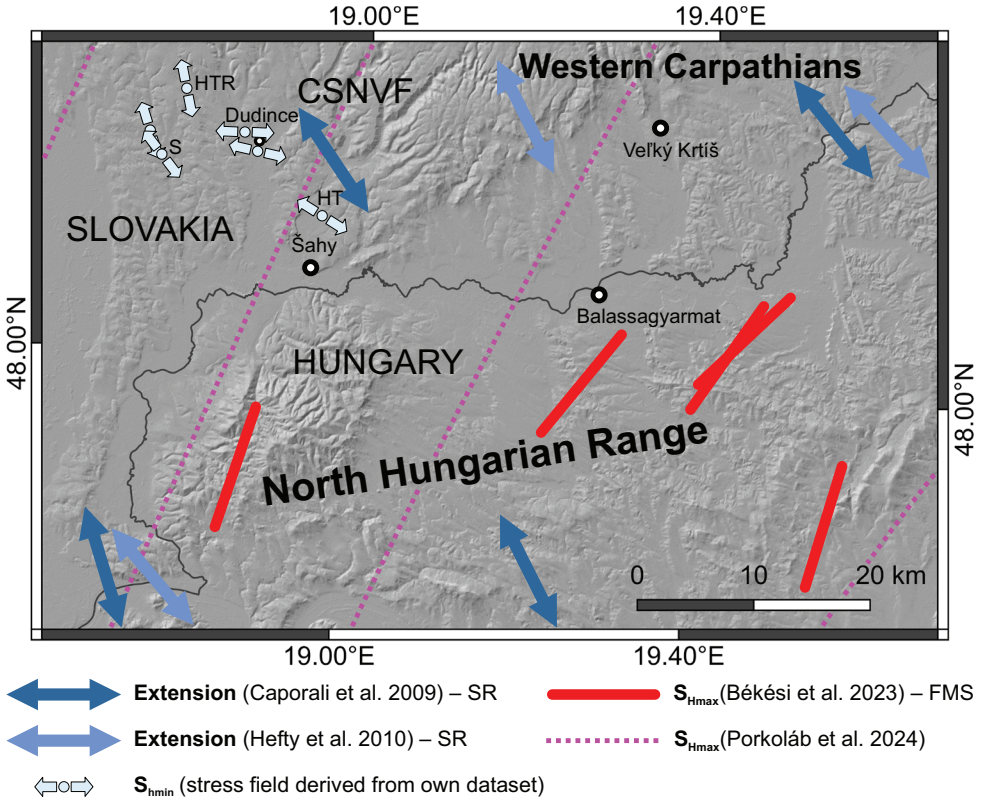

Fig. 12. Minimum regional horizontal stress (S_{hmin}) acting within the current tectonic regime on contact between the Western Carpathians and the North Hungarian Range. Explanations: SR – strain rate, FMS – focal mechanism solutions, S – Santovka village, HTR – Hontianske Trsťany village, HT – Horné Turovce village, CSNVF – Central Slovak Neogene volcanic field.

was most likely a consequence of the persistent back-arc extension. Our deformational phase – D1 (Figs. 9 and 11) was active during the Middle Pleistocene, when there was a significant reorientation of the direction of extension towards the northeast–southwest.

In the Upper Pleistocene and Holocene, the extension was generally oriented parallel to the IWECA arc, with its orientation oscillating from SW–NE to WNW–ESE, confirming the extension parallel orogen in the western parts of the IWECA region. These findings contrast somewhat with the results of Németh et al. (2023). It is probable that the orientation of S_{hmin} is partly determined by the location of the studied area in the Central Slovak Fault System (CSFS) zone and its persistent dextral transtension regime.

Unfortunately, the Middle Pleistocene covers a relatively long period of time (0.774–0.129 Ma), making it difficult to determine the time of change more precisely.

In Dudince, numerical ages were obtained from the Tatársky prameň Spring travertine (No. 7) 301,072±18,317 yr BP and the travertines from the Močidlá site (Grófsky kúpeľ Spring No. 10) 25,853±2124 yr BP (Vieira et al. 2023; Fig. 2). The results of the research on travertines from northern Hungary show an extension orientation in the NE–SW direction (Török et al. 2019), and their numerical age has been determined to be 553±60 ka to 318±18 ka. The problem lies in the interpretation of U/Th data, which show different values than biostratigraphic or historical data (Ruszkiczay-Rüdiger et al. 2020). From the above data, we can tentatively deduce that a radical reorientation of paleostress tension from the NW–SE (deformational phase – D1, Figs. 9 and 11) to the NE–SW (deformational phase – D2, Figs. 9 and 11) occurred later than 553±60 ka, and the consequent reorientation is not younger than 25,853±2124 yr BP.

The NNW–SSE to WNW–ESE orientation of the minimum horizontal stress vector (S_{hmin}) during the youngest deformational phase – D3 (Würm (Weichselian)–Holocene – Figs. 9, 11 and 12) aligns with the present-day orientation of the maximum horizontal stress trajectories (S_{Hmax}) derived from the focal mechanism solutions (Békési et al. 2023; Porkoláb et al. 2024). Our observations are also consistent with the directions of the main deformational axes (strain rate) in recent surface kinematics in Central Europe (see fig. 7 in Caporali et al. 2009) and partially in Slovakia (see fig. 13 in Hefty et al. 2010).

The change in stress orientation during the Quaternary period raises the question of the correct definition of neotectonics for the IWECA area. In the Western Carpathians, the term neotectonics referred to tectonic processes that took place from the end of the Miocene to the present (Hók et al. 2000; Kováč et al. 2002; Vojtko et al. 2008, 2011), although it was later suggested to modify this definition (Littva & Hók 2014; Hók et al. 2016). If we were to narrow down the definition of neotectonics within the studied area, but also within

the IWECA area, to the period that has elapsed since the last tectonic reorganization and continues to the present (Şengör et al. 1985; Muir Wood & Mallard 1992), it would correspond to the Late Pleistocene–Recent period. In this case, it is better to use the term "current tectonic regime" as recommended, for example, in the International Atomic Energy Agency's safety standards (IAEA 2010) for seismic hazard assessment.

The integration of field research with LiDAR data, GIS spatial analysis, and 3D point cloud analysis has provided a comprehensive, multi-dimensional understanding of the terrain and geological features of the Dudince Spa and surroundings. This methodological approach has not only enhanced the identification of key spatial attributes of travertine geobodies for further field study, but has also established a solid foundation for accurately interpreting the geological evolution, particularly concerning the tectonic influences on travertine formation.

Morphometric analysis shows that the fine forms of the travertine lobes remain well-preserved on the mound surfaces. This preservation implies a subrecent age, as older forms (depo-shapes) would likely have been degraded by erosion.

In this study, we also tested the relationship between neotectonic systematic joints and the orientation of the main trends of morpholineaments obtained by extraction from the system of gullies. Our results show a positive spatial correlation between them. The main trends of morpholineament concentrations (Fig. 7A, B) are parallel to the measured systematic joints (Fig. 7G, H).

Conclusions

Findings from our new geological mapping of the Dudince Spa indicate that travertine geobodies are considerably less extensive than those in older geological maps. Lithologically, we recognised two types of terrestrial carbonates: (i) compact grey-white to light-brown travertine and (ii) porous, layered, often crumbly travertine, somewhere with the lithified flora residues.

Based on structural, paleostress analysis, and according to principles of travitonics, we derived Quaternary stress field orientation at individual localities, such as the Dudince Spa and Gestenec area, Dudince village – Under the vineyards (Porošín), the Búr River valley and Santovka Spa, the village of Hontianske Trsťany – quarry, and the village of Horné Turovce – quarry.

We attribute the origin travertine/tufa and their brittle deformations to the tectonic movements of the CSFS within an dextral transtension tectonic regime during the Quaternary. We concluded that during the Quaternary, the extension in the Internal Western Carpathians progressively changed the orientation from the NW–SE (deformational phase – D1), to the NE–SW (ENE–WSW, deformational phase – D2), and finally to the ESE–WNW or SSE–NNW (deformational phase – D3). The progressive reorientation of extension, from a generally NW–SE to ENE–WSW towards an ESE–WNW (SSE–NNW) direction, was generated by dextral movement along the CSFS during the Mindel (Elsterian)–Holocene period. A thorough understanding of this final phase of extension is essential for characterising the present-day stress field. In many aspects, this study refines the youngest phase of deformation identified by Németh et al. (2023) and Németh (2024) for the Western Carpathians region.

This study provides new insights into neotectonic activity in the region, as well as their implications for the management of low-thermal mineral water resources, particularly in areas affected by active tectonics. The origin and circulation of mineral waters are interpreted as being associated with the Bzovík Depression northeast of Dudince.

The erosional pattern of gullies correlates with the orientation of joint patterns that formed during the Middle to Late Pleistocene.

By using geomorphometric analyses, we have demonstrated how the effective and unambiguous identification of travertine mounds as distinct geomorphological forms. This approach is transferable to other environments, where such features may not have been previously recognised. In open environments like deserts, terrain modelling can be effectively carried out using photogrammetry. However, in regions with dense forest or shrub cover, where vegetation obscures the underlying terrain, LiDAR remains the only reliable method for capturing subtle landforms with high precision. Our results underscore the broader applicability of this method for identifying small-scale geomorphological features across diverse landscapes.

Finally, the geological and structural results presented here should be considered in the selection process for future deep geological repository sites for radioactive waste disposal in Slovakia (Slaninka et al. 2007).

Acknowledgements: The work was financially supported by the Slovak Research and Development Agency under contract Nos. APVV-21-0281, APVV-22-0024, APVV-20-0120 and by the Scientific Grant Agency of the Ministry of Education, Research, Development and Youth of the Slovak Republic (VEGA) under No. 1/0780/24. Thanks to Dr. Mariana Kováčová for the identification of flora remains in the tufa. The authors also thank the handling editor Dr. I. Broska for his editing and comments, and also the reviewers Dr. P. Štěpančíková, Prof. L.I. Fodor and Dr. D. Pivko for their constructive comments and manuscript improvement.

References

Abou Elmagd K., Fathy A.H.M., Abdelwahab W. & Younis M.H. 2024: Tectonic and climate changes influences on distribution and morphology of Quaternary travertine, Kurkur oasis, Egypt. *Journal of African Earth Sciences* 218, 105365. https://doi.org/10.1016/j.jafrearsci.2024.105365

Ahmadi H. & Pekkan E. 2021: Fault-based geological lineaments extraction using remote sensing and GIS – a review. *Geosciences* 11, 183. https://doi.org/10.3390/ geosciences11050183

Altunel E. 2005: Travertines: neotectonic indicators. In: Özkul M., Yagiz S. & Jones B. (Eds): Travertine. Proceedings of 1st International Symposium on Travertine, September 21–25, 2005, Denizli-Turkey. *Kozan Ofset*, Ankara, 120–127.

Altunel E. & Hancock P.L. 1993: Active Fissuring and Faulting in Quaternary Travertines at Pamukkale, Western Turkey. *Zeitschrift für Geomorphologie, Suppl. Iss.* 94, 285–302.

Altunel E. & Karabacak V. 2005: Determination of horizontal extension from fissure-ridge travertines: a case study from the Denizli Basin, southwestern Turkey. *Geodinamica acta* 18, 333–342. https://doi.org/10.3166/ga.18.333-342

Andrić-Tomašević N., Simić V., Životić D., Nikolić N., Pavlović A., Kluge T., Beranoaguirre A., Smit J. & Bechtel A. 2024: Tectonically induced travertine deposition in the Middle Miocene Levač intramountain basin (Central Serbia). *Sedimentology* 71, 1214–1244. https://doi.org/10.1111/sed.13171

Angelier J. 1994: Fault Slip Analysis and Palaeostress Reconstruction. In: Hancock P.L. (Ed.): Continental Deformation. *Pergamon Press,* Oxford, New York, 53–100.

Bačová N., Ženišová Z. & Michalko J. 2015: Chemical composition of mineral water in Dudince, Santovka and Slatina. *Podzemná voda* 21, 63–82 (in Slovak with English summary).

Bačová N., Németh Z. & Repčiak M. 2016: Mineral waters of the Dudince Spa. *Slovak Geological Magazine* 16, 125–147.

Békési E., Porkoláb K., Wesztergom V. & Wéber Z. 2023: Updated stress dataset of the Circum-Pannonian region: implications for regional tectonics and geo-energy applications. *Tectonophysics* 856, 229860. https://doi.org/10.1016/j.tecto.2023.229860

Biela A. 1978: Hlboké vrty v zakrytých oblastiach vnútorných Západných Karpát. *Regionálna Geológia Západných Karpát* 11, 8–224.

Bóna J., Gallay M., Macková A., Bónová K., Littva J. & Hók J. 2024: Travertine and calcareous tufa occurrences as an indicator of the ongoing tectonic activity of the Central Slovak Fault System inferred from airborne laser scanning data, geomorphometric, and structural analysis (Northern Slovakia). *Geomorphology* 466, 109420. https://doi.org/10.1016/j.geomorph.2024.109420

Bondarenková Z. 1983: Hydrogeological and hydrochemical experience from prospection in the Santovka source area [Hydrogeologické a hydrogeochemické poznatky z prieskumných prác v Santovke]. *Mineralia Slovaca* 15, 347–361 (in Slovak with English summary).

Briestenský M. 2008: Indikátory zlomovej aktivity Brezovskej časti Malých Karpát [Fault activity indicators of the Malé Karpaty Mts. Brezová part]. *Geomorphologia Slovaca et Bohemica* 8, 16–25 (in Slovak with English abstract).

Brilli M. & Giustini F. 2023: Geochemical stratigraphy of the Prima Porta travertine deposit (Roma, Italy). *Minerals* 13, 789. https://doi.org/10.3390/min13060789

Brogi A. 2004: Faults linkage, damage rocks and hydrothermal fluid circulation: tectonic interpretation of the Rapolano Terme travertines (southern Tuscany, Italy) in the context of Northern Apennines Neogene–Quaternary extension. *Eclogae Geologicae Helvetiae* 97, 307–320. https://doi.org/10.1007/s00015-004-1134-5

Brogi A. & Capezzuoli E. 2009: Travertine deposition and faulting: the fault-related travertine fissure-ridge at Terme S. Giovanni, Rapolano Terme (Italy). *International Journal of Earth Sciences* 98, 931–947. https://doi.org/10.1007/s00531-007-0290-z

Brogi A., Capezzuoli E. & Gandin A. 2007: Travertines at Terme San Giovanni (Rapolano Terme, Northern Apennines) and their neotectonic implications. *Il Quaternario – Italian Journal of Quaternary Sciences* 20, 107–124 (in Italian with English summary). https://amq.aiqua.it/index.php/amq/article/view/398

Brogi A., Capezzuoli E., Aqué R., Branca M. & Voltaggio M. 2010: Studying travertines for neotectonics investigations: Middle–Late Pleistocene syn-tectonic travertine deposition at Serre di Rapolano (Northern Apennines, Italy). *International Journal of Earth Sciences* 99, 1383–1398. https://doi.org/10.1007/s00531-009-0456-y

Brogi A., Capezzuoli E., Buracchi E. & Branca M. 2012: Tectonic control on travertine and calcareous tufa deposition in a low-temperature geothermal system (Sarteano, Central Italy). *Journal of the Geological Society* 169, 461–476. https://doi.org/10.1144/0016-76492011-137

Brogi A., Capezzuoli E., Kele S., Baykara M.O. & Shen C.C. 2017: Key travertine tectofacies for neotectonics and palaeoseismicity reconstruction: effects of hydrothermal overpressured fluid injection. *Journal of the Geological Society* 174, 679–699. https://doi.org/10.1144/jgs2016-124

Brogi A., Liotta D., Capezzuoli E., Matera P.F., Kele S., Soligo M., Tuccimei P., Ruggieri G., Yu T.L., Shen C.C. & Huntington K.W. 2020: Travertine deposits constraining transfer zone neotectonics in geothermal areas: An example from the inner Northern Apennines (Bagno Vignoni-Val d'Orcia area, Italy). *Geothermics* 85, 101763. https://doi.org/10.1016/j.geothermics.2019.101763

Brogi A., Capezzuoli E., Karabacak V., Alcicek M.C. & Luo L. 2021: Fissure Ridges: A Reappraisal of Faulting and Travertine Deposition (Travitonics). *Geosciences* 11, 278. https://doi.org/10.3390/geosciences11070278

Burian L., Šujan M., Stankoviansky M., Šilhavý J. & Okai A. 2017: Dependence of gully networks on faults and lineaments networks, case study from Hronska Pahorkatina Hill Land. *Open Geosciences* 9, 101–113. https://doi.org/10.1515/geo-2017-0008

Capezzuoli E. & Sandrelli F. 2006: Neotectonic evidence in the Quaternary continental carbonates from Southern Valdelsa Basin (Tuscany). *Il Quaternario – Italian Journal of Quaternary Sciences* 19, 155–166. https://amq.aiqua.it/index.php/amq/article/view/449

Capezzuoli E., Ruggieri G., Rimondi V., Brogi A., Liotta D., Alçiçek M.C., Alçiçek H., Bülbül A., Gandin A., Meccheri M., Shen C.-C. & Baykara M.O. 2018: Calcite veining and feeding conduits in a hydrothermal system: insights from a natural section across the Pleistocene Gölemezli travertine depositional system (western Anatolia, Turkey). *Sedimentary Geology* 364, 180–203. https://doi.org/10.1016/j.sedgeo.2017.12.012

Caporali A., Aichhorn C., Barlik M., Becker M., Fejes I., Gerhatova L., Ghitau D., Grenerczy G., Hefty J., Krauss S., Medak D., Milev G., Mojzes M., Mulic M., Nardo A., Pesec P., Rus T., Simek J., Sledzinski J., Solaric M., Stangl G., Stopar B., Vespe F. & Virag G. 2009: Surface kinematics in the Alpine–Carpathian–Dinaric and Balkan region inferred from a new multi-network GPS combination solution. *Tectonophysics* 474, 295–321. https://doi.org/10.1016/j.tecto.2009.04.035

Claes H., Soete J., Van Noten K., El Desouky H., Marques Erthal M., Vanhaecke F., Özkul M. & Swennen R. 2015: Sedimentology, three-dimensional geobody reconstruction and carbon dioxide origin of Pleistocene travertine deposits in the Ballık area (southwest Turkey). *Sedimentology* 62, 1408–1445. https://doi.org/10.1111/sed.12188

Coe A.L., Argles T.W., Rothery D.A. & Spicer R.A. 2010: Geological field techniques. *Wiley-Blackwell,* London, 1–323.

Çolak Erol S., Özkul M., Aksoy E., Kele S. & Ghaleb B. 2015: Travertine occurrences along major strike-slip fault zones: Structural, depositional and geochemical constraints from the Eastern Anatolian Fault System (EAFS), Turkey. *Geodinamica Acta* 27, 155–174. https://doi.org/10.1080/09853111.2014.979530

Cox R.T., Van Arsdale R.B. & Harris J.B. 2001: Identification of possible Quaternary deformation in the northeastern Mississippi Embayment using quantitative geomorphic analysis of drainage-basin asymmetry. *Geological Society of America Bulletin* 113, 615–624. https://doi.org/10.1130/0016-7606(2001)113<0615:IOPQDI>2.0.CO;2

Dabkowski J. 2014: High potential of calcareous tufas for integrative multidisciplinary studies and prospects for archaeology in Europe. *Journal of Archaeological Science* 52, 72–83. https://doi.org/10.1016/j.jas.2014.07.013

DeLong S.B., Hilley G.E., Rymer M.J., Prentice C. 2010: Fault zone structure from topography: Signatures of en echelon fault slip at Mustang Ridge on the San Andreas fault, Monterey County, California. *Tectonics* 29, TC5003. https://doi.org/10.1029/2010TC002673

Dramis F., Materazzi M. & Cilla G. 1999: Influence of climatic changes on freshwater travertine deposition: a new hypothesis. *Physics and Chemistry of the Earth, Part A: Solid Earth and Geodesy* 24, 893–897. https://doi.org/10.1016/S1464-1895(99)00132-5

Dunne W.M. & Hancock P.L. 1994: Palaeostress Analysis of Small-Scale Brittle Structures. In: Hancock P.L. (Ed.): Continental Deformation. *Pergamon Press,* Oxford, New York, 101–120.

Dzúrik J., Tomana J. & Hók J. 2021: Prehodnotenie ochrany prírodných liečivých zdrojov v Dudinciach a prírodných minerálnych zdrojov v Santovke a v Slatine. Záverečná správa z doplnkového hydrogeologického prieskumu. *Open file report — Geofond,* Bratislava, 1–124 (in Slovak).

EDF & Telecom ParisTech 2007: CloudCompare [Software]. CloudCompare 3D point cloud and mesh processing software Open Source Project. *EDF & TELECOM ParisTech,* Paris, France. Available on web: http://www.danielgm.net/cc/ (accessed on 1 November 2023)

Ekizoğlu Ö. & Mesci B.L. 2025: Morphotectonic and active tectonic properties of the Yenicekent travertines with Chibanian–Meghalayan ages in the Denizli graben (Türkiye). *Turkish Journal of Earth Sciences* 34, 630–649. https://doi.org/10.55730/1300-0985.1980

Evans I.S. 1972: General Geomorphometry, Derivations of Altitude and Descriptive Statistics. In: Chorley R.J. (Ed.): Spatial Analysis in Geomorphology. *Methuen & Co. Ltd.,* London, 17–90.

Evans I.S. & Minár J. 2011: A classification of geomorphometric variables. In: Hengl T., Evans I.S., Wilson J.P. & Gould, M. (Eds.): Proceedings of Geomorphometry 2011. *International Society for Geomorphometry, International Society for Geomorphometry,* Redlands, 105–108.

Faccenna C., Soligo M., Billi A., De Filippis L., Funiciello R., Rossetti C. & Tuccimei P. 2008: Late Pleistocene depositional cycles of the Lapis Tiburtinus travertine (Tivoli, Central Italy): possible influence of climate and fault activity. *Global and Planetary Change* 63, 299–308.

Florinsky I.V. 1996: Quantitative topographic method of fault morphology recognition. *Geomorphology* 16, 103–119. https://doi.org/10.1016/0169-555X(95)00136-S

Florinsky I.V. 2016: Digital terrain analysis in soil science and geology. *Academic Press*, Amsterdam, 1–486.

Florinsky I.V. 2017: An illustrated introduction to general geomorphometry. *Progress in Physical Geography* 41, 723–752. https://doi.org/10.1177/0309133317733667

Florinsky I.V. 2023: Larsemann Hills: Geomorphometric modeling and mapping. *Polar Science* 38, 100969. https://doi.org/10.1016/j.polar.2023.100969

Ford T.D. & Pedley H.M. 1996: A review of tufa and travertine deposits of the world. *Earth-Science Reviews* 41, 117–175. https://doi.org/10.1016/S0012-8252(96)00030-X

Fornaciai A., Favalli M., Karátson D., Tarquini S. & Boschi E. 2012: Morphometry of scoria cones, and their relation to geodynamic setting: A DEM-based analysis. *Journal of Volcanology and Geothermal Research* 217, 56–72. https://doi.org/10.1016/j.jvolgeores.2011.12.012

Franko O. 2001: Origin and development of mineral and thermal waters of Slovakia in space and time from the view of the age of travertines and ^{18}O, H and ^{14}C isotopes. *Podzemná Voda* VII, 26–45 (in Slovak with English summary).

Gazda S. 1971: Modification of the Palmer classification system [Modifikácia Palmerovho klasifikačného systému]. *Hydrogeological yearbook (Hydrogeologická ročenka)* 1970–1971, 56–79 (in Slovak).

Geological Map 2008: Digital Geological Map of the Slovak Republic at scale 1:50,000 (accessed 08/2008, last update 01/2024). *State Geological Institute of Dionýz Štúr,* Bratislava. Available on web: http://apl.geology.sk/gm50js

Gradziński M., Wróblewski W., Duliński M. & Hercman H. 2014: Earthquake-affected development of a travertine ridge. *Sedimentology* 61, 238–263. https://doi.org/10.1111/sed.12086

GRASS Development Team 2020: Geographic Resources Analysis Support System (GRASS) Software, Version 7.8. *Open Source Geospatial Foundation Project.* https://grass.osgeo.org

Guyot A., Hubert-Moy L. & Lorho T. 2018: Detecting Neolithic burial mounds from LiDAR-derived elevation data using a multi-scale approach and machine learning techniques. *Remote Sensing* 10, 225. https://doi.org/10.3390/rs10020225

Halouzka R. 1977: Contribution to the stratigraphy of the travertines from the Ipeľská pahorkatina upland. *Geologické Práce, Správy* 67, 135–140. (in Slovak with English summary)

Hancock P.L. 1968: Joints and faults: The morphological aspects of their origins. *Proceedings of the Geologists' Association* 79, 141–151. https://doi.org/10.1016/S0016-7878(68)80032-X

Hancock P.L. 1991: Determining contemporary stress directions from neotectonic joint systems. *Philosophical Transactions of the Royal Society of London – Series A: Physical and Engineering Sciences* 337, 29–40. https://doi.org/10.1098/rsta.1991.0104

Hancock P.L. & Engelder T. 1989: Neotectonic joints. *Geological Society of America Bulletin* 101, 1197–1208. https://doi.org/10.1130/0016-7606(1989)101<1197:NJ>2.3.CO;2

Hancock P.L. & Chalmers R.M.L., Altunel E. & Ćakir Z. 1999: Travitonics: using travertines in active fault studies. *Journal of Structural Geology* 21, 903–916. https://doi.org/10.1016/S0191-8141(99)00061-9

Heddi M., Eastaff D.J. & Petch J. 1999: Relationships between tectonic and geomorphological linear features in the Guadix-Baza basin, southern Spain. *Earth Surface Processes and Landforms* 24, 931–942. https://doi.org/10.1002/(SICI)1096-9837(199909)24:10<931::AID-ESP27>3.0.CO;2-V

Hefty J., Hipmanová, L., Gerhátová Ľ., Igondová M. & Droščák B. 2010: Recent geo-kinematics of Slovakia based on homogenised solutions of permanent and epoch GPS networks. *Acta Geodynamica et Geomaterialia* 7, 303–315.

Hofierka J., Mitasova H. & Neteler M. 2009: Geomorphometry in GRASS GIS. In: Hengl T. & Reuter H.I. (Eds.): Geomorphometry: Concepts, Software, Applications. Developments in Soil Science. *Elsevier,* Amsterdam, 387–410. https://doi.org/10.1016/S0166-2481(08)00017-2

Hók J., Bielik M., Kováč P. & Šujan M. 2000: Neotectonic character of Slovakia. *Mineralia Slovaca* 32, 459–470 (in Slovak with English summary).

Hók J., Kysel R., Kováč M., Moczo P., Kristek J., Kristekova M. & Šujan M. 2016: A seismic source zone model for the seismic hazard assessment of Slovakia. *Geologica Carpathica* 67, 273–288. https://doi.org/10.1515/geoca-2016-0018

Hók J., Šujan M., Sýkora M. & Šipka F. 2020: Geology and tectonics of the Levice-Santovka elevation (southwest margin of the Štiavnica stratovolcano). *Geologické práce, Správy* 135, 47–50 (in Slovak with English summary).

Hók J., Šujan M., Král M., Pelech O. & Šipka F. 2021: Pre-Cenozoic basement of the eastern part of the Danube Basin. *Geologické práce, Správy* 137, 3–18.

Hyánková K. & Melioris L. 1993: The unusual chemism of mineral wates at Dudince. *Geologica Carpathica* 44, 123–131.

Hynie O. 1956a: Celkové vyhodnocení výsledků prací v lázích Dudince od jejich začátku do dokončení vrtu S-4 s návrhem plánu daších vrtů až do konečného využití zřídel. *Open file report — Archive of MH SR,* Bratislava (in Czech).

Hynie O. 1956b: Nové jímání minerální vody v lázních Dudincích u Levic na jižním Slovensku [Die neue fassung der Mineralwässer im Bad Dudince bei Levice (Südslowakei)]. *Universitas Carolina, Geologica* 2, 1–23 (in Czech with German summary).

Hynie O. 1963: Hydrogeologie ČSSR II. Minerální vody. *ČSAV,* Praha, 1–797.

IAEA 2010: Seismic hazards in site evaluation for nuclear installations, IAEA Safety Standards – Series N, SSG-9. *IAEA*, Vienna, 1–78.

Ivan Ľ. 1943: Výskyty travertínov na Slovensku [Die Travertinvorkommen in der Slowakei]. *Práce Štátneho geologického Ústavu Sošit 9,* 1–71 (in Slovak with German summary)

Ivan Ľ. 1952: Geologická stavba a minerálne premene okolia Levíc [Der geologische Bau und die Mineralquellen in der Umgebung von Levice]. *Geologické práce, Sošit* 32, 5–22 (in Slovak with German summary).

Jordan G. 2007: Adaptive smoothing of valleys in DEMs using TIN interpolation from ridgeline elevations: an application to morphotectonic aspect analysis. *Computers & Geosciences* 33, 573–585. https://doi.org/10.1016/j.cageo.2006.08.010

Kania M. & Szczęch M. 2023: Tectonic structures interpretation using airborne-based LiDAR DEM on the examples from the Polish Outer Carpathians. In: Misra A.A., Mukherjee S. (Eds.): Atlas of Structural Geological and Geomorphological Interpretation of Remote Sensing Images. John Wiley & Sons, Oxford, 157–166.

Konečný V. (Ed.), Lexa J., Halouzka R., Hók J., Vozár J., Dublan L., Nagy A., Šimon L., Havrila M., Ivanička J., Hojstričová V., Miháliková A., Vozárová A., Konečný P., Kováčiková M., Filo M., Marcin D., Klukanová A., Liščák P. & Žáková E. 1998: Geologická mapa Štiavnických vrchov a Pohronského Inovca (štiavnický stratovulkán) v mierke 1:50 000 [Geological map of Štiavnické vrchy Mts. and Pohronský Inovec Mts. (Štiavnica stratovolcano) in scale 1:50,000]. *Ministerstvo životného prostredia SR – Geologická služba SR,* Bratislava.

Konečný V., Lexa J. & Šimon L. 2003: Geologic structure and evolution of intravolcanic depressions in the area of Neogene volcanism in central Slovakia. *Mineralia Slovaca* 35, 255–290.

Kováč M., Bielik M., Hók J., Kováč P., Kronome B., Labák P., Moczo P., Plašienka D., Šefara J., Šujan M. 2002: Seismic activity and neotectonic evolution of theWestern Carpathians (Slovakia). In: Cloetingh S.A.P.L., Horváth F., Bada G., Lankreije A.C. (Eds.): Neotectonics and surface processes: the Pannonian Basin and Alpine/Carpathian System. *Stephan Mueller Spec. Publ. Ser.* 3, *Copernicus,* 167–184. https://doi.org/10.5194/smsps-3-167-2002

Kováč P. & Hók J. 1993: The Central Slovak Fault System – the field evidence of a strike slip. *Geologica Carpathica* 44, 155–159.

Kovanda J. 1971: Quaternary limestones of Czechoslovakia. *Sborník geologických věd, Antropozoikum* A7, 7–236 (in Czech with English summary).

Krcho J. 1973: Morphometric analysis of relief on the basis of geometric aspect of field theory. *Acta Geographica Universitatis Comenianae, Geographico-Physica* 1, 7–233.

Krcho J. 1983: Teoretická koncepcia a interdisciplinárne aplikácie komplexného digitálneho modelu reliéfu pri modelovaní dvojdimenzionálnych polí. [Theoretical conception and interdisciplinary applications of the complex digital model of relief in modeling bidimensional fields]. *Geografický časopis* 35, 265–291 (in Slovak with English abstract and summary).

Krcho J. 1990: Morphometric analysis and Digital Models of Georelief. *VEDA,* Bratislava, 1–427 (in Slovak with English summary).

Lačný A., Vojtko R., Dušeková L. & Čahojová L. 2024: Dolines as important indicators of lithology and tectonics: A case study of the Malé Karpaty Mts. (Western Carpathians). *Acta Geologica Slovaca* 16, 79–97.

Lin Z., Kaneda H., Mukoyama S., Asada N. & Chiba T. 2013: Detection of subtle tectonic–geomorphic features in densely forested mountains by very high-resolution airborne LiDAR survey. *Geomorphology* 182, 104–115. https://doi.org/10.1016/j.geomorph.2012.11.001

Littva J. & Hók J. 2014: Neotectonics of the Inner Western Carpathians: Liptovský Ján area, case study northern slopes of the Nízke Tatry Mts., Slovakia). *Acta Geologica Slovaca* 6, 123–134.

Littva J., Hók J. & Bella P. 2015: Cavitonics: using caves in active tectonic studies (Western Carpathians, case study). *Journal of Structural Geology* 80, 47–56. https://doi.org/ 10.1016/j.jsg.2015.08.011

Maheľ M. 1952: Slané vody pri okraji Krupinskej vrchoviny. *Geologické práce, Sošit* 32, 23– 30 (in Slovak with German summary).

Mancini A., Capezzuoli E., Erthal M. & Swennen R. 2019: Hierarchical approach to define travertine depositional systems: 3D conceptual morphological model and possible applications. *Marine and Petroleum Geology* 103, 549–563. https://doi.org/10.1016/j.marpetgeo.2019.02.021

Mancini A., Della Porta G., Swennen R. & Capezzuoli E. 2021: 3D reconstruction of the Lapis Tiburtinus (Tivoli, Central Italy): The control of climatic and sea-level changes on travertine deposition. *Basin Research* 33, 2605–2635. https://doi.org/10.1111/bre.12576

Marko F., Reichwalder P., Jablonský J. & Vojtko R. 2007: Metódy terénneho geologického výskumu. Geologické mapovanie. *Vydavateľstvo UK*, Bratislava, 1–110.

Marková M., Planderová E. & Polák M. 1972: Oligocene evaporites in Central West Carpathians. *Geologický Zborník, Geologica Carpathica* 23, 263–280.

Melioris L. & Vass D. 1982: Hydrogeologické a geologické pomery levickej žriedelnej línie. *Západné Karpaty – Séria hydrológia, inžinierska geológia, geotermálna energia* 4, 7–56.

Melioris L., Hyánková K., Pospíšil P., Böhm V., Fendeková M., Čech P., Mucha I., Némethy P., Paulíková E., Ženišová Z., Glesková E., Pokorná L., Purašová A., Sramelová M., Malatinský K. & Beracko I. 1986: Dudince – Santovka – Slatina. Záverečná správa z vyhľadávacieho hydrogeologického prieskumu. *Open file report – Geofond,* Bratislava, 1–188 (in Slovak).

Mesci B.L. 2012: Active tectonics of the Ortaköy fissure-ridge-type travertines: implications for the Quaternary stress state of the neotectonic structures of the Central Anatolia, Turkey. *Geodinamica Acta* 25, 12–25. https://doi.org/10.1080/09853111.2013.813744

Mesci B.L., Gürsoy H. & Tatar O. 2008: The evolution of travertine masses in the Sivas Area (Central Turkey) and their relationships to active tectonics. *Turkish Journal of Earth Sciences* 17, 219–240. https://journals.tubitak.gov.tr/earth/vol17/iss2/2

Minár J. & Feciskanin R. 2024: Geomorfometria I – Úvod do geomorfometrie a všeobecná geomorfometria [Geomorphometry I – Introduction to Geomorphometry and General Geomorphometry]. *Univerzita Komenského v Bratislave*, Bratislava, 1–92.

Minár J. & Sládek J. 2009: Morphological network as an indicator of a morphotectonic field in the central Western Carpathians (Slovakia). *Zeitschrift für Geomorphologie, Suppl. Iss.* 53, 23–29. https://doi.org/10.1127/0372-8854/2009/0053S3-0023

Minár J., Evans I.S. & Jenčo M. 2020: A comprehensive system of definitions of land surface (topographic) curvatures, with implications for their application in geoscience modelling and

prediction. *Earth-Science Reviews* 211, 103414. https://doi.org/10.1016/j.earscirev.2020.103414

Minár J., Drăguț L., Evans I. S., Feciskanin R., Gallay M., Jenčo M. & Popov A. 2024: Physical geomorphometry for elementary land surface segmentation and digital geomorphological mapping. *Earth-Science Reviews* 248, 104631. https://doi.org/10.1016/j.earscirev.2023.104631

Mitášová H. & Hofierka J. 1993: Interpolation by regularized spline with tension: II. Application to terrain modeling and surface geometry analysis. *Mathematical Geology* 25, 657–669. https://doi.org/10.1007/BF00893172

Mohammadi Z., Capezzuoli E., Claes H., Alipoor R., Muchez P. & Swennen R. 2019: Substrate geology controlling different morphology, sedimentology, diagenesis and geochemistry of adjacent travertine bodies: A case study from the Sanandaj-Sirjan zone (western Iran). *Sedimentary Geology* 389, 127–146. https://doi.org/10.1016/j.sedgeo.2019.06.005

Muir Wood R. & Mallard D.J. 1992: When a fault is 'extinct'? *Journal of the Geological Society* 149, 251–254. https://doi.org/10.1144/gsjgs.149.2.0251

Nagy A. (Ed.), Halouzka R., Konečný V., Dublan L., Havrila M., Lexa J. & Pristaš J. 1998: Geologická mapa Podunajskej nížiny – východná časť v mierke 1: 50 000. [Geological map of the Danube Lowland – Eastern part in scale 1:50,000]. *Ministerstvo životného prostredia SR – Geologická služba SR,* Bratislava.

Nemcok M., Hok J., Kovac P., Marko F., Coward M.P., Madaras J., Houghton J.J. & Bezak V. 1998: Tertiary extension development and extension/compression interplay in the West Carpathian mountain belt. *Tectonophysics* 290, 137–167. https://doi.org/10.1016/S0040-1951(98)00016-X

Németh Z. 2024: Geodynamics of polyorogenic zones: Case study from the Western Carpathians. *Mineralia Slovaca* 56, 103–142. https://doi.org/10.56623/ms.2024.56.2.1

Németh Z., Maglay J., Petro Ľ., Stercz M., Grega D., Pelech O. & Gaál Ľ. 2023: Neo-Alpine uplift and subsidence zones in the Western Carpathians: Product of kinematic activity on Cenozoic AnD3 (NW–SE and NE–SW) and AnD4 (E–W – subequatorial and N–S – submeridian) regional faults. *Mineralia Slovaca* 55, 103–116. https://doi.org/10.56623/ms.2023.55.2.1

Nishikawa O., Furuhashi K., Masuyama M., Ogata T., Shiraishi T. & Shen C.C. 2012: Radiocarbon dating of residual organic matter in travertine formed along the Yumoto Fault in Oga Peninsula, northeast Japan: implications for long-term hot spring activity under the influence of earthquakes. *Sedimentary Geology* 243, 181–190. https://doi.org/10.1016/j.sedgeo.2011.11.001

Özkul M., Gökgöz A., Kele S., Baykara M.O., Shen C.C., Chang Y.W. Kaya, A. Hancer M., Aratman C., Akin T. & Örü Z. 2014: Sedimentological and geochemical characteristics of a fluvial travertine: a case from the eastern Mediterranean region. *Sedimentology* 61, 291–318. https://doi.org/10.1111/sed.12095

Pánek T., Minár J., Vitovič L. & Březný M. 2020: Post-LGM faulting in Central Europe: LiDAR detection of the >50 km-long Sub-Tatra fault, Western Carpathians. *Geomorphology* 364, 107248. https://doi.org/10.1016/j.geomorph.2020.107248

Pedersen G.B.M. & Grosse P. 2014: Morphometry of subaerial shield volcanoes and glaciovolcanoes from Reykjanes Peninsula, Iceland: Effects of eruption environment. *Journal of Volcanology and Geothermal Research* 282, 115–133. https://doi.org/10.1016/j.jvolgeores.2014.06.008

Pentecost A. 2005: Travertine. *Springer-Verlag*, Berlin, 1–445.

Petit J.P. 1987: Criteria for the sense of movement on fault surfaces in brittle rocks. *Journal of structural Geology* 9, 597–608. https://doi.org/10.1016/0191-8141(87)90145-3

Pike R.J. 1988: The geometric signature: quantifying landslide-terrain types from digital elevation models. *Mathematical geology* 20, 491–511. https://doi.org/10.1007/BF00890333

Pilous V. 1973: Závrty v travertínech v Dudincích. *Československý kras* 24, 123–125.

Pivko D. 2021: A review of Slovak travertine and tufa facies and their environment. *Acta Geologica Slovaca* 13, 129–166.

Pivko D. & Vojtko R. 2021: A review of travertines and tufas in Slovakia: Geomorphology, environments, tectonic pattern, and age distribution. *Acta Geologica Slovaca* 13, 49–78.

Porkoláb K., Békési E., Győri E., Broerse T., Czecze B., Kenyeres A., Tari G. & Wéber Z. 2024: Present-day stress field, strain rate field and seismicity of the Pannonian region: overview and integrated analysis. In: Tari G.C., Kitchka A., Krézsek C., Lučić D., Markič M., Radivojević D., Sachsenhofer R.F. & Šujan M. (Eds.): The Miocene Extensional Pannonian Superbasin, Volume 1: Regional Geology. *Geological Society, London, Special publications* 554. 1–25. https://doi.org/10.1144/SP554-2023-219

QGIS Development Team 2020: QGIS Geographic Information System. *Open Source Geospatial Foundation Project.* http://qgis.osgeo.org

Ricketts J.W., Ma L., Wagler A.E. & GarciaV.H. 2019: Global travertine deposition modulated by oscillations in climate. *Journal of Quaternary Science* 34, 558–568. https://doi.org/10.1002/jqs.3144

Ruszkiczay-Rüdiger Z., Balázs A., Csillag G., Drijkoningen G. & Fodor L. 2020: Uplift of the Transdanubian Range, Pannonian Basin: how fast and why? *Global and Planetary Change* 192, 103263. https://doi.org/10.1016/j.gloplacha.2020.103263

Sales J.C., Bueno G.T., Rosolen V., Ferreira M.E. & Furlan L.M. 2021: The structure of an earth-mound field of the Brazilian Savanna. *Geomorphology* 386, 107752. https://doi.org/10.1016/j.geomorph.2021.107752

Schäfer D., Heinrich W.-D., Böhme G. & Steiner W. 2007: Aspects of the geology, palaeontology and archaeology of the travertine sites of Weimar-Ehringsdorf (Thuringia, Central Europe). In: Kahlke R.-D., Maul L.Ch. & Mazza P.P.A. (Eds.): Late Neogene and Quaternary biodiversity and evolution: Regional developments and interregional correlations. *Courier Forschungsinstitut Senckenberg* 259, *E. Schweizerbart,* Stuttgart, 141–147.

Scheidegger A.E. & Ai N.S. 1986: Tectonic processes and geomorphological design. *Tectonophysics* 126, 285–300. https://doi.org/10.1016/0040-1951(86)90234-9

Scheuer G. & Schweitzer F. 1985: Types and forms of travertine cones. *Földtani Közlöny* 115, 385–398 (in Hungarian with English summary).

Schmidt Z. 1977: Geographical extension of archidiscodonts in Slovakia. *Západné Karpaty – Séria paleontológia* 23, 233–240.

Scholz C.H. 2002: The Mechanics of Earthquakes and Faulting. *Cambridge University Press*, New York, 1–471. https://doi.org/10.1017/CBO9780511818516

Şengör A.M.C., Görür N. & Şaroğlu F. 1985: Strike-slip faulting and related basin formation in zones of tectonic escape: Turkey as a case study. In: Biddle K.T. & Christie-Blick N. (Eds.): Strike-slip Deformation, Basin Formation, and Sedimentation. *Society of Economic Paleontologists and Mineralogists, Special Publication* 37, Tulsa, 227–264.

Şengül M.A., Gürboğa Ş., Akkaya İ. & Özvan A. 2019: Deformation patterns in the Van region (Eastern Turkey) and their significance for the tectonic framework. *Geologica Carpathica* 70, 193–208. https://doi.org/10.2478/geoca-2019-0011

Shary P.A. 1995: Land surface in gravity points classification by a complete system of curvatures. *Mathematical Geology* 27, 373–390. https://doi.org/10.1007/BF02084608

Shebl A. & Csámer Á. 2021: Reappraisal of DEMs, Radar and optical datasets in lineaments extraction with emphasis on the spatial context. *Remote Sensing Applications: Society and Environment* 24, 100617. https://doi.org/10.1016/j.rsase.2021.100617

Slaninka I., Hók J. & Franzen J. 2007: Vývoj a stav hlbinného úložiska RAO v Slovenskej Republike z hľadiska geologického poznania [Status and development of deep geological repository in Slovak republic from geological point of view]. *Acta Montanistica Slovaca* 12, *Special Issue* 1, 17–23.

Šolcová A., Jamrichová E., Horsák M., Pařil P., Petr L., Heiri O., Květoň J., Křížek M., Hartvich F., Hájek M. & Hájková P. 2020: Abrupt vegetation and environmental change since the MIS 2: a unique paleorecord from Slovakia (Central Europe). *Quaternary Science Reviews* 230, 106170.

Stewart I.S. & Hancock P.L. 1994: Neotectonics. In: Hancock P.L. (Ed.): Continental Deformation. *Pergamon Press,* Oxford, New York, 370–409.

Sun W., Wei Z., Sun H. & He H. 2022: Review on the application of airborne LiDAR in active tectonics of China: Dushanzi reverse fault in the Northern Tian Shan. *Frontiers in Earth Science* 10, 895758. https://doi.org/10.3389/feart.2022.895758

Tkáčová H. 1978: Geofyzikálny prieskum levickej žriedelnej línie, oblasť Dudince – Slatina. Záverečná správa. *Open file report – Geofond,* Bratislava, 1–19 (in Slovak).

Török Á., Mindszenty A., Claes H., Kele S., Fodor L. & Swennen R. 2017: Geobody architecture of continental carbonates: "Gazda" travertine quarry (Süttő, Gerecse Hills, Hungary). *Quaternary International* 437, 164–185. https://doi.org/10.1016/j.quaint.2016.09.030

Török Á., Claes H., Brogi A., Liotta D., Tóth Á., Mindszenty A., Kudó I., Kele S., Huntington K.W., Shen C.C. & Swennen R. 2019: A multi-methodological approach to reconstruct the configuration of a travertine fissure ridge system: The case of the Cukor quarry (Süttő, Gerecse Hills, Hungary). *Geomorphology* 345, 106836. https://doi.org/10.1016/j.geomorph.2019.106836

Uysal I.T., Feng Y., Zhao J.X., Altunel E., Weatherley D., Karabacak V., Cengiz O., Golding S.D., Lawrence M.G. & Collerson K.D. 2007: U-series dating and geochemical tracing of late Quaternary travertine in co-seismic fissures. *Earth and Planetary Science Letters* 257, 450–462. https://doi.org/10.1016/j.epsl.2007.03.004

Van Noten K., Claes H., Soete J., Foubert A., Özkul M. & Swennen R. 2013: Fracture networks and strike–slip deformation along reactivated normal faults in Quaternary travertine deposits, Denizli Basin, western Turkey. *Tectonophysics* 588, 154–170. https://doi.org/10.1016/j.tecto.2012.12.018

Van Noten K., Topal S., Baykara M.O., Özkul M., Claes H., Aratman C. & Swennen R. 2019: Pleistocene-Holocene tectonic reconstruction of the Ballık travertine (Denizli Graben, SW Turkey): (De)formation of large travertine geobodies at intersecting grabens. *Journal of Structural Geology* 118, 114–134. https://doi.org/10.1016/j.jsg.2018.10.009

Vandrová G., Matejčeková E. & Bujalka P. 1988: Dudince – zdroj minerálnej vody S-5/A a likvidácia S-5. Záverečná správa z doplnkového hydrogeologického prieskumu. *Open file report – Geofond,* Bratislava, 1–50 (in Slovak).

Vandrová G., Matejčeková E. & Dudáš J. 1990a: Dudince – zdroj minerálnej vody HVD-1, Záverečná správa z hydrogeologického prieskumu. *Open file report – Geofond,* Bratislava, 1–26 (in Slovak).

Vandrová G., Matejčeková E. & Dudáš J. 1990b: Dudince – zdroj minerálnej vody HVD-2. Záverečná správa z vyhľadávacieho hydrogeologického prieskumu. *Open file report – Geofond,* Bratislava, 1–25 (in Slovak).

Vass D. 1971: Sedimentological characterisation of the Plášťovce beds (Southern Slovakia). *Geologický zborník – Geologica Carpathica* 22, 25–47.

Vass D., Began A., Gross P., Kahan Š., Köhler E., Lexa J. & Nemčok J. 1988a: Regionálne geologické členenie Západných Karpát a severných výbežkov Panónskej panvy na území ČSSR v mierke 1:500 000. *Slovenský geologický úrad*, *Geologický Ústav Dionýza Štúra – Geofond*, Bratislava.

Vass D., Began A., Gross P., Kahan Š., Krystek I., Köhler E., Lexa J., Nemčok J., Růžička M. & Vaškovský I. 1988b: Vysvetlivky k mape: Regionálne geologické členenie Západných Karpát a severných výbežkov Panónskej panvy na území ČSSR v mierke 1:500 000. *Geologický Ústav Dionýza Štúra,* Bratislava, 1–65.

Vass D., Hók J., Kováč P. & Elečko M. 1993: The Paleogene and Neogene tectonic events of the Southern Slovakia depressions in the light of the stress-field analyses. *Mineralia Slovaca* 25, 79–92.

Veselský M., Lačný A. & Hók J. 2014: Závrty na Dlhom vrchu: modelová štúdia ich vzniku na lineárnych diskontinuitách (Malé Karpaty) [Dolines on Dlhý vrch Hill: case study of doline evolution on linear discontinuity (Malé Karpaty Mts.)]. *Acta Geologica Slovaca 6,* 59–168. (in Slovak with English summary)

Vieira D.S.C., Pivko D., Rinyu L., Palcsu L., Kiss G.I., Hu H.-M., Shen C.-C. & Kele S. 2023: Age and depositional temperature of Quaternary travertine spring mounds from Slovakia. *Minerals* 13, 794. https://doi.org/10.3390/min13060794

Vinci G. & Vanzani F. 2025: Bronze Age monumental earthworks of the Friuli Plain (NE Italy): from LiDAR-based morphometric analysis to the reconstruction of settlement patterns and organization. *Archaeological and Anthropological Sciences* 17, 19. https://doi.org/10.1007/s12520-024-02127-w

Viveen W., van Balen R.T., Schoorl J.M., Veldkamp A., Temme A.J.A.M. & Vidal-Romani J.R. 2012: Assessment of recent tectonic activity on the NW Iberian Atlantic Margin by means of geomorphic indices and field studies of the Lower Miño River terraces. *Tectonophysics* 544, 13–30. https://doi.org/10.1016/j.tecto.2012.03.029

Vojtko R., Hók J., Kováč M., Sliva Ľ., Joniak P., Šujan M. 2008: Pliocene to Quaternary stress field change in western part of Central Western Carpathians (Slovakia). *Geological Quarterly* 52, 19–30.

Vojtko R., Beták J., Hók J., Marko F., Gajdoš V., Rozimant K. & Mojzeš A. 2011: Pliocene to Quaternary tectonics in the Horná Nitra Depression (Western Carpathians). *Geologica Carpathica* 62, 381–393. https://doi:10.2478/v10096-011-0028-5

Wachtel D. 1859: Ungarns Kurorte und Mineralquellen. *Bei Sering & Hennicke,* Oedenberg, 1–475.

Whitbread K., Thomas C. & Finlayson A. 2024: The influence of bedrock faulting and fracturing on sediment availability and Quaternary slope systems, Talla, Southern Uplands, Scotland, UK. *Proceedings of the Geologists' Association* 135, 61–77. https://doi.org/10.1016/j.pgeola.2023.11.003

Wood J. 1996: The Geomorphological Characterisation of Digital Elevation Models. *PhD Thesis, University of Leicester*, UK, 1–456.

Yokoyama R., Shirasawa M. & Pike R.J. 2002: Visualizing topography by openness: A new application of image processing to digital elevation models. *Photogrammetric Engineering & Remote Sensing* 68, 257–266.

Yong Technology Inc. 2014: GeoRose [Software]. *Yong Technology Inc.,* Edmonton (AB), Canada. Available on web: http://www.yongtechnology.com/download/georose

Zakšek K., Oštir K. & Kokalj Ž. 2011: Sky-view factor as a relief visualization technique. *Remote Sensing* 3, 398–415. https://doi.org/10.3390/rs3020398

ZBGIS Map Client 2017: A web application, which serves for work with ZBGIS data (accessed 07/2017, last update 04/2023). *Office of Geodesy, Cartography and Cadastre of the Slovak Republic – ÚGKK SR,* Bratislava. Available on web: https://zbgis.skgeodesy.sk/mkzbgis/sk/teren